Virtual Tire Test Rig

Mathematical Model Formulation

Nicolas Romanella

18 November 2026

Version 1.6

Abstract

This report describes the model of a virtual test rig for one wheel with its tire, the first subsystem of a Vehicle Dynamics Simulator. The rig imposes the road speed with a moving belt and steers the wheel through any angle, while drive and brake torques act on the rim. The model combines the kinematics of the rolling wheel, an isotropic tire law built on the PAC2002 Magic Formula, the spin dynamics of the rim and a transient tire with carcass damping that remains valid down to standstill. It returns the tire forces and moments, the spin and the actions at the hub. The rig characterizes the tire and verifies the wheel as a subsystem before it is implemented in the simulator. All parameters come from one published wheel, the Project Chrono sedan wheel. The report states the assumptions and limitations of each part of the model, the numerical solution, and a verification plan of scenarios with acceptance criteria. The model is implemented in Python and passes every scenario of the plan; numbers not tied to a scenario are hand calculations or come from the scripts named in the text.

Contents

Nomenclature **3**

1 Introduction **5**
1.1 Purpose . . . 5
1.2 Scope . . . 5
1.3 Sources . . . 5

2 Test rig **5**
2.1 Imposed road speed . . . 5
2.2 Frames and sign conventions . . . 6
2.3 Inputs, parameters, states and outputs . . . 6
2.4 Parameters . . . 7
2.5 Assumptions . . . 8
2.6 Interface to the simulator . . . 8

3 Kinematics **9**
3.1 Wheel velocity . . . 9
3.2 Rolling radius and free-rolling spin . . . 9
3.3 Rolling conditions . . . 10
3.4 Slip velocity . . . 11
3.5 Slip indices . . . 12

4 Tire model **13**
4.1 Direction of the force on an isotropic tire . . . 13
4.2 Characteristic . . . 14
4.3 Practical slip in the characteristic . . . 15
4.4 Combined slip . . . 16
4.5 Pure slip and load . . . 16
4.6 Rolling resistance . . . 18
4.7 Aligning moment . . . 19

5 Wheel dynamics **23**
5.1 Masses, load and radii . . . 23
5.2 Free-body diagram and balance . . . 23
5.3 Hub actions . . . 24
5.4 Spin equation and torque inputs . . . 25
5.5 Stability under torque input . . . 26

6 Transient tire **26**
6.1 Purpose . . . 26
6.2 Maxwell model . . . 27
6.3 Low-speed problem . . . 28
6.4 Carcass damping . . . 28
6.5 Parameters . . . 30
6.6 Growth of the transient slip in sliding . . . 30

7 Numerical solution **30**
7.1 State equations . . . 30
7.2 Integrator and time step . . . 31
7.3 Controls and reset . . . 31

8 Verification plan **32**
8.1 Reference values 32
8.2 Scenarios 32
8.3 Results 33

9 Limitations and future work **34**
9.1 Limitations 34
9.2 Future work 34
9.3 Evidence gaps 35

References **36**

Nomenclature

Symbol	Quantity	Unit
B, C, D, E	Magic Formula factors	–, –, N, –
B_t, C_t, D_t, E_t	trail factors	–, –, m, –
C_s	slip stiffness of the isotropic tire	N
C_x, C_α	longitudinal and cornering stiffness	N
F_σ	the characteristic written in $\boldsymbol{\sigma}$	N
c	contact damper, $C_s/\lvert V_x\rvert$	N s/m
c_0	carcass damping	N s/m
c_z	vertical stiffness of the tire	N/m
d, d_{eff}	relaxation length, effective value	m
df_z	load change, $(F_z - F_{z0})/F_{z0}$	–
e	forward offset of the vertical load	m
$\mathbf{e}_r$, $\mathbf{e}_n$, $\mathbf{e}_z$	belt direction, its normal, vertical	–
F_x, F_y, F_z	road forces on the tire	N
$\mathbf{F}_t$, F_t	tangential road force, its size	N
$F_\parallel, F_\perp$	tire force along and across the belt	N
F_{z0}, F_{nom}	scaled nominal load $\lambda_{Fz0}F_{nom}$, nominal load of the file	N
f, f_0, K_f	rolling-resistance coefficient, parameters	–, –, s^2/m^2
h	loaded radius, height of the hub	m
g	gravitational acceleration	m/s^2
J_w	spin inertia of the wheel	kg m^2
K	carcass stiffness	N/m
κ	longitudinal slip of PAC2002, $-s_x$	–
ℓ	distance rolled	m
λ_{Fz0}	load scaling factor of the tire file	–
m_w	mass of the wheel	kg
M_x, M_y, M_z	overturning, rolling-resistance, aligning moment	N m
$\mathbf{M}_h$, M_{hx}, M_{hz}	moment of the frame at the hub	N m
P	vertical load on the fork, a test condition	N
$p_{\ldots}$, $q_{\ldots}$	coefficients of the tire file, Tables 4.1 and 4.2	–
$\mathbf{q}$	states (Ω, τ_x, τ_y)	–
R, R_0, R_e	rolling, free-rolling, unloaded radius	m
$\mathbf{R}_h$, R_{hx}, R_{hy}, R_{hz}	force of the frame at the hub	N
$\mathbf{s}$, $\boldsymbol{\sigma}$	practical and theoretical slip	–
s, σ	size of the practical and theoretical slip	–
T, T_D, T_B	net, drive and brake torque	N m
T_f	friction torque of brake and rolling resistance	N m
T_h	torque to be held by a wheel at rest	N m
T_{lock}, T_{max}	locking torque, torque limit	N m
t	pneumatic trail	m
u, u_k, u_c	displacement of the rim, of the carcass, of the patch	m
V, $\mathbf{V}$	belt speed, velocity of the wheel center	m/s
V_0	belt speed at the start of a scenario	m/s
V_x, V_y	components of $\mathbf{V}$ in the wheel frame	m/s
$\mathbf{V}_r$, $\mathbf{V}_s$	rolling velocity, slip velocity	m/s
α, α_t	slip angle, slip input of the trail $\lvert\tan\alpha\rvert$	rad, –
α_p	slip angle at the peak lateral force	rad
δ	steer angle relative to the belt	rad

Symbol	Quantity	Unit
θ	direction of the slip from x	rad
μ_0, μ_1	peak and sliding friction coefficients	–
ν	direction of the friction torque, ± 1, 0 when held	–
ρ	vertical deflection of the tire	m
σ_p, s_p	slip at the peak force	–
$\boldsymbol{\tau}$, $\boldsymbol{\tau}^*$	transient slip, slip to the characteristic	–
Ω	spin of the rim	rad/s
Ω_0, $\Omega_{0\alpha}$	free-rolling spin at zero and at α	rad/s
Ω_s	spin scale of the smooth sign, rejected in Section 5.4	rad/s
ω_n	natural frequency of the spin–tire mode	rad/s

1 Introduction

1.1 Purpose

This work is the first step of a Vehicle Dynamics Simulator, a vehicle model that runs in real time and is driven through inputs from outside, by a person, a controller or an optimiser. Once the simulator is complete, a controller and machine-learning algorithms will be developed on it to find the minimum lap time.

The simulator is built one subsystem at a time, starting from the wheel. The wheel carries every force between the vehicle and the road, so its tire must be characterized and verified before anything is built on it. This report describes a virtual test rig for one wheel with its tire. The rig has two purposes. The first is to characterize the tire. Each combination of inputs gives one steady operating point, so the force and moment curves of the tire can be read directly. The second is to verify the wheel as a subsystem. The rig gives the wheel its velocity, as the chassis will do in the simulator, and the wheel returns its forces and its spin. A wheel that passes the verification of Section 8 is then implemented in the simulator without changes.

1.2 Scope

The rig covers every rolling condition of a wheel on a flat road, namely free rolling, pure lateral slip, braking, driving, locking, wheel spin and their combinations. It also covers two conditions outside the usual range of a tire model. One is a wheel steered past 90° that rolls backward, the other a belt brought to rest with the wheel held by the tire. The transient build-up of the tire force is included.

The model does not represent camber, vertical dynamics, temperature, pressure or wear. The load can be changed by the user, but it reaches the tire at once, without dynamics. The longitudinal behavior of the tire is taken equal to its lateral behavior. These and the other limitations are collected in Section 9.

1.3 Sources

Notation and theory follow the lecture notes of A. De Felice [1]. Every tire parameter comes from one published wheel, the sedan wheel of Project Chrono [2]. Its PAC2002 tire file, for a 245/40 R18 tire, gives the Magic Formula coefficients, the radii, the vertical stiffness and the relaxation length, and the Chrono rim and tire files give mass and inertia. The only exception is rolling resistance, for which the file has no coefficients. The PAC2002 formulation is that of H. B. Pacejka [3].

Statements that are not derived carry one of four labels. An estimate is a hand calculation, a design choice is a decision without a measured basis, a hypothesis is a plausible but unchecked statement, and verified marks the result of a named test that has run.

2 Test rig

2.1 Imposed road speed

To characterize a tire, each set of inputs must give one steady operating point. The rig therefore imposes the road speed, as flat-track tire testing machines do. The hub is held by a fixed frame and a flat belt runs under the wheel at the imposed speed V, Figure 2.1. A constant torque and a constant steer angle then bring the wheel to a steady spin, so the slip and the forces become constant and can be read.

A vertical fork holds the axle. Its stem runs in a cylindrical joint fixed to the frame, so the fork can turn about the vertical axis through the contact point O and slide along it. The controller turns the fork by the steer angle δ from the belt direction $\mathbf{e}_r$. The belt moves at $-V\mathbf{e}_r$, so the wheel center moves relative to the road surface at $\mathbf{V} = V\mathbf{e}_r$. The belt drive supplies whatever force keeps V, so the tire cannot change it. The frame presses the fork down with a constant vertical load P.

The input is the steer angle and not the slip angle because the slip angle is undefined when the belt is at rest, while the steer angle is always defined. For $V > 0$ the two are equal, Section 3.1.

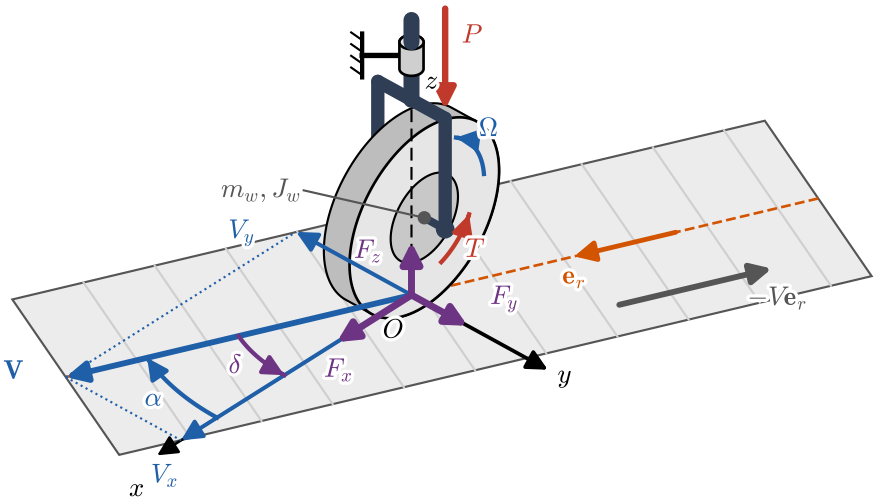


Figure 2.1. The rig. The fork is turned by δ from the belt direction $\mathbf{e}_r$ to the wheel axis x and pressed down by the load P. The belt runs at $-V\mathbf{e}_r$, so the wheel center moves at $\mathbf{V} = V\mathbf{e}_r$ relative to the road; its wheel-frame components V_x and V_y are drawn at O. All quantities in their positive direction.

2.2 Frames and sign conventions

The wheel frame $(O; x, y, z)$ has its origin at the center of the contact patch, x forward in the mid-plane of the wheel, y to the left along the axle and z up, Figure 2.2. Frame and belt direction are fixed, so this is the only frame of the model. Units are SI, angles in radians.

The steer angle δ is measured from $\mathbf{e}_r$ to x, positive counter-clockwise seen from above, that is with the wheel turned to the left; $\delta \in (-\pi, \pi]$. The slip angle α is measured from x to $\mathbf{V}$, positive clockwise seen from above. With $\alpha > 0$ the wheel moves to its right and the tire gives $F_y > 0$, to the left. The spin Ω is positive when the wheel rolls forward; a positive torque drives and a negative torque brakes.

2.3 Inputs, parameters, states and outputs

Table 2.1 lists the variables of the model by role. The inputs come from the controls, Section 7.3, and may change at any moment. The test conditions are set by the user and usually held constant; V may be changed during a run, up to 70 m/s, a design choice, and a new V or P keeps states and inputs, the tire following the new load at once, A3. The parameters are fixed by the wheel, Section 2.4. The states are integrated in time, Section 7; the outputs are computed at each step and never integrated. The slip angle is therefore an output; for $V > 0$ it equals δ, Equation (3.2), and the memory of the tire lies in the transient slip $\boldsymbol{\tau}$, Section 6.

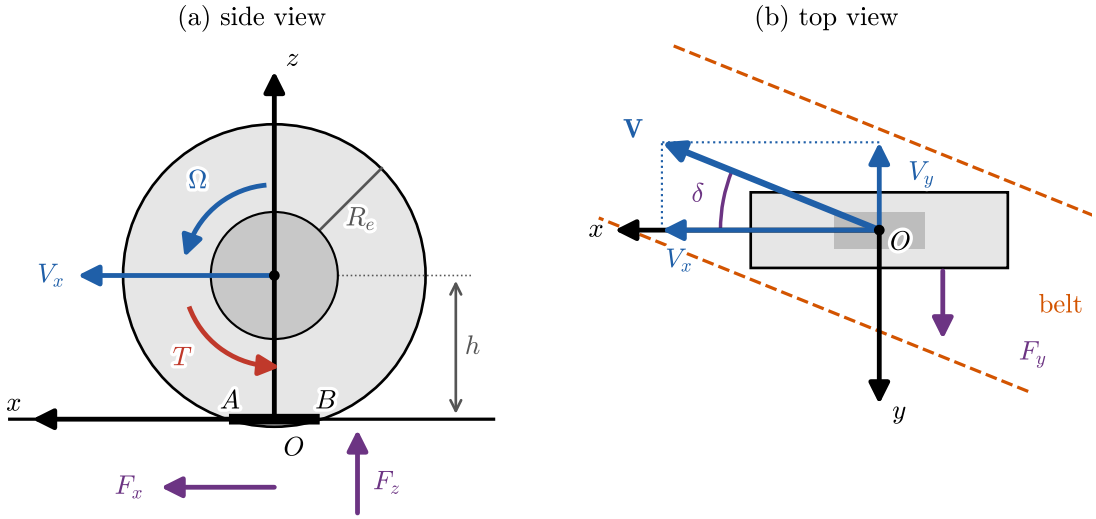


Figure 2.2. Wheel frame and sign conventions. (a) Side view, x to the left and z up, with loaded radius h, unloaded radius R_e, contact patch AB around O, spin Ω, torque T and the road forces F_x and F_z. (b) Top view, x to the left, y down and z toward the reader, with the road force F_y. The belt fixes the direction of $\mathbf{V}$ and the wheel is turned by δ from the belt to x; here $\alpha = \delta > 0$, so $V_y < 0$ and the wheel moves to its right. All quantities in their positive direction.

Role	Quantity	Symbol	Unit
input	steer angle	δ	rad
input	drive torque	T_D	N m
input	brake torque	T_B	N m
test condition	belt speed, 0 to 70 m/s	V	m/s
test condition	vertical load on the fork	P	N
state	spin of the rim	Ω	rad/s
state	transient slip	τ_x, τ_y	–
output	slip angle, rolling radius	α, R	rad, m
output	wheel and slip velocity	V_x, V_y, $\mathbf{V}_s$	m/s
output	slip indices	$\mathbf{s}$, $\boldsymbol{\sigma}$	–
output	tire forces and moments	F_x, F_y, M_y, M_z	N, N m
output	hub force and moment	$\mathbf{R}_h$, $\mathbf{M}_h$	N, N m

Table 2.1. Variables of the model by role.

2.4 Parameters

Table 2.2 lists every parameter of the model with its origin. The tire parameters depend on the contact load F_z and are evaluated at the current load at every time step; the table gives them at the reference load $F_z = 2.70$ kN, about a quarter of the weight of an 1100 kg car, and the sections given as source derive them. The load P can be set between 1.72 and 5.65 kN, so that F_z stays between $0.5F_{z0}$ and $1.5F_{z0}$, that is 1.96 to 5.89 kN. This range lies within the limits of 225 N and 10.1 kN given in the tire file [2]; the file does not state the loads it was fitted on.

Quantity	Symbol	Value	Source
wheel mass	m_w	24.7 kg	Chrono rim and tire [2]
spin inertia	J_w	1.10 kg m^2	Chrono rim and tire [2]
reference load on the fork	P	2.46 kN	design choice
reference contact load	F_z	2.70 kN	$P + m_w g$, Section 5.1
scaled nominal load	F_{z0}	3930 N	$\lambda_{Fz0} F_{nom}$, tire file [2]
unloaded radius	R_e	0.344 m	tire file [2]
vertical stiffness	c_z	281 kN/m	tire file [2]
loaded radius	h	0.334 m	Section 5.1
free-rolling radius	R_0	0.341 m	Section 5.1
slip stiffness	C_s	52.9 kN	tire file, Section 4.5
peak and sliding friction	μ_0, μ_1	1.105, 0.942	tire file, Section 4.5
rolling resistance	f_0, K_f	0.015, $5.2 \cdot 10^{-7}$ s^2/m^2	[1], [4]
trail at zero slip	D_t	22.8 mm	tire file, Table 4.2
relaxation length	d	0.370 m	tire file, Section 6.5
carcass stiffness	K	143 kN/m	C_s/d
carcass damping	c_0	233 N s/m	design choice

Table 2.2. Parameters of the model at the reference load.

2.5 Assumptions

The model rests on the following assumptions. They define its validity domain and are referred to by number in the rest of the report.

- A1 The frame is fixed and rigid. The belt runs along a fixed direction at the imposed speed $V \geq 0$, and δ changes only through the controller.
- A2 The belt is flat, the camber is zero and the wheel stays vertical.
- A3 The rim is rigid and the tire deformable. The contact load $F_z = P + m_w g$ follows the load P at once, so there are no vertical dynamics, and the tire parameters are evaluated at the current F_z.
- A4 The radii R_0 and h are constant, computed once at the reference load, Section 5.1. In reality both depend on F_z, V and α.
- A5 The tire gives F_x, F_y, the rolling-resistance moment M_y and the aligning moment M_z. The overturning moment M_x is zero; it is kept as a symbol in the balance equations.
- A6 The tire is isotropic and grips the same in every direction, Section 4.1.
- A7 The wheel is axisymmetric with its center of mass at the hub and spin inertia J_w. Its steering inertia and the gyroscopic moment are neglected, Section 5.2.
- A8 There are no aerodynamic, temperature, pressure or wear effects.

2.6 Interface to the simulator

In the simulator, at each time step the chassis will give each hub its velocity and load, as the belt and the fork do on the rig, and the wheel will return the derivatives of its states, its forces and its hub actions. The wheel is therefore the same function on the rig and in the simulator,

$$(V_x,\ V_y,\ F_z,\ T_D,\ T_B,\ \nu;\ \Omega,\ \boldsymbol{\tau}) \longrightarrow (\dot{\Omega},\ \dot{\boldsymbol{\tau}};\ F_x,\ F_y,\ M_y,\ M_z,\ \mathbf{R}_h,\ \mathbf{M}_h) \tag{2.1}$$

Here $\mathbf{R}_h$ and $\mathbf{M}_h$ are the force and the moment of the frame on the wheel at the hub, with the components of Section 5.3, and ν is the direction of the friction torque, zero for a held wheel;

how it is decided at each time step is given in Section 7.2, and the simulator applies the same rule to each wheel.

The rig leaves out the loop of the vehicle, in which the tire force changes the chassis speed and the speed changes the slip (limitation L1). Turning the chassis motion into V_x and V_y at each wheel belongs to the simulator.

3 Kinematics

3.1 Wheel velocity

$\mathbf{V} = V\mathbf{e}_r$ is the velocity of the wheel center relative to the belt, and x is turned by δ from $\mathbf{e}_r$, Figure 2.2b. In the wheel frame $\mathbf{e}_r = (\cos\delta, -\sin\delta)$, so for every δ

$$V_x = V\cos\delta, \qquad V_y = -V\sin\delta \tag{3.1}$$

The tire literature writes the same components with the slip angle, $V_x = V\cos\alpha$ and $V_y = -V\sin\alpha$ [1]. Hence, for $V > 0$,

$$\alpha = \delta \tag{3.2}$$

The tire equations below are written with α, as they will be in the simulator, where α follows from the chassis motion; δ is kept for the rig. At $V = 0$ the slip angle is undefined. Only the trail of the aligning moment uses it and takes $\alpha = 0$ there, Section 4.7; every other equation uses only V_x, V_y and Ω. Table 3.1 shows that the same equations cover every steer angle, with no special case above 90°.

Case	δ	α	Motion of the wheel
straight	0	0	rolls forward
turned left	20°	20°	moves to its right, $F_y > 0$
sideways	90°	90°	slides along its axle, $V_x = 0$
reversed	180°	180°	rolls backward, $V_x < 0$, $\Omega < 0$

Table 3.1. Examples of steer angle and resulting motion.

3.2 Rolling radius and free-rolling spin

The motion of the rim is a rotation Ω about an axis whose trace C lies on the vertical through the wheel center, at the distance

$$R = \frac{V_x}{\Omega} \tag{3.3}$$

below it. The free-rolling radius R_0 is the value of R when no torque acts. It differs from the unloaded radius R_e and from the hub height h because the tire is deformed. By A4, R_0 does not depend on α. The free-rolling spin is then

$$\Omega_{0\alpha} = \frac{V\cos\alpha}{R_0} = \Omega_0\cos\alpha, \qquad \Omega_0 = \frac{V}{R_0} \tag{3.4}$$

The wheel rolls freely at the spin that matches the speed along its own plane. This spin is below Ω_0 with a slip angle, zero at $\alpha = 90°$ and $-\Omega_0$ at $\alpha = 180°$.

3.3 Rolling conditions

The points on the vertical through the wheel center move along x at $\Omega(z - z_C)$, zero at C and V_x at the center. The position of C therefore tells what the wheel is doing. The side views of Figures 3.1 to 3.4 show the x components; with a slip angle the sideways slip $V_{sy} = V_y$ is perpendicular to the page.

In free rolling, $\alpha = 0$ and $T = 0$, Figure 3.1. Then $\Omega = \Omega_0$, $R = R_0$ and C coincides with the point C_0 of the tire at depth R_0. The contact point does not slide and there is no force.

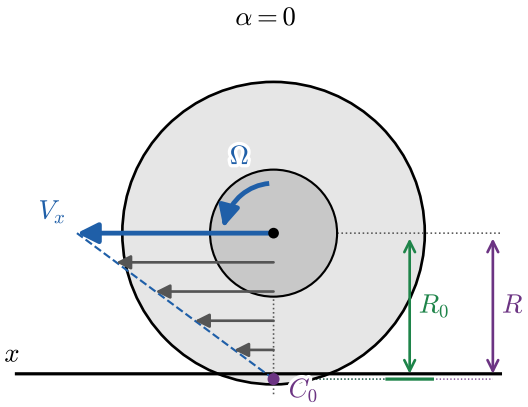


Figure 3.1. Free rolling, with $\Omega = \Omega_0$, $R = R_0$ and $C = C_0$. The contact point does not slide.

In pure slip, $\alpha \neq 0$ and $T = 0$, Figure 3.2. Along x the wheel still rolls freely, $\Omega = \Omega_{0\alpha}$ and $V_{sx} = 0$; across it the contact point slides at $V_{sy} = -V \sin\alpha$, which gives the lateral force.

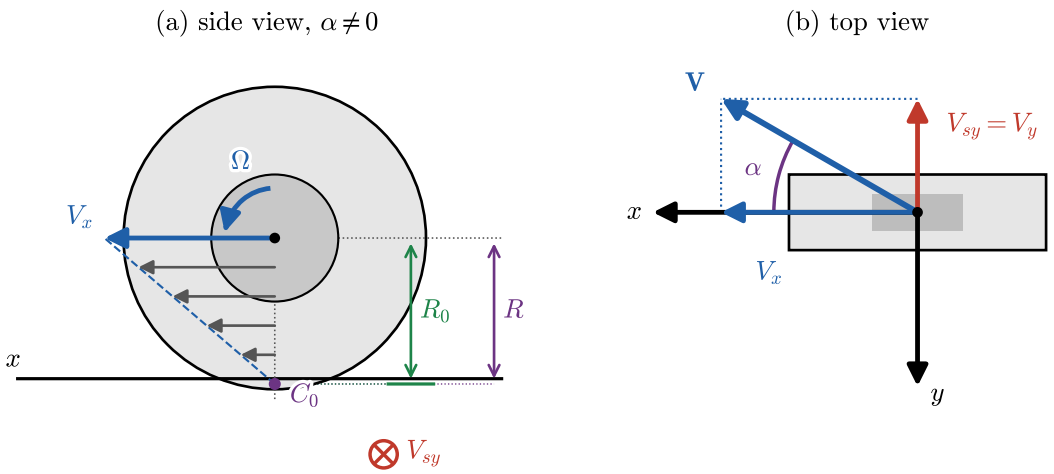


Figure 3.2. Pure slip. (a) Side view. The center moves along x at $V\cos\alpha$ with $C = C_0$, so there is no slip along x; the contact point slides sideways, V_{sy} into the page. (b) Top view, with $\mathbf{V}$ split into V_x and $V_y = V_{sy}$.

With a torque, $T \neq 0$, the spin moves away from $\Omega_{0\alpha}$ and the contact point also slides along x; with $\alpha \neq 0$ this is combined slip. A braked wheel, $T < 0$, spins at $\Omega < \Omega_{0\alpha}$, Figure 3.3. Then $R > R_0$ and C lies below the road; the contact point slides forward, $V_{sx} > 0$, and the force acts backward. In the limit of a locked wheel $\Omega \to 0$, $R \to \infty$ and the wheel translates. A driven wheel, $T > 0$, spins at $\Omega > \Omega_{0\alpha}$, Figure 3.4. Then $R < R_0$ and C lies above C_0; the contact

point slides backward, $V_{sx} < 0$, and the force acts forward. The limit of a wheel spinning on the spot, $V_x = 0$, is reached at $V = 0$ with the transient tire of Section 6.

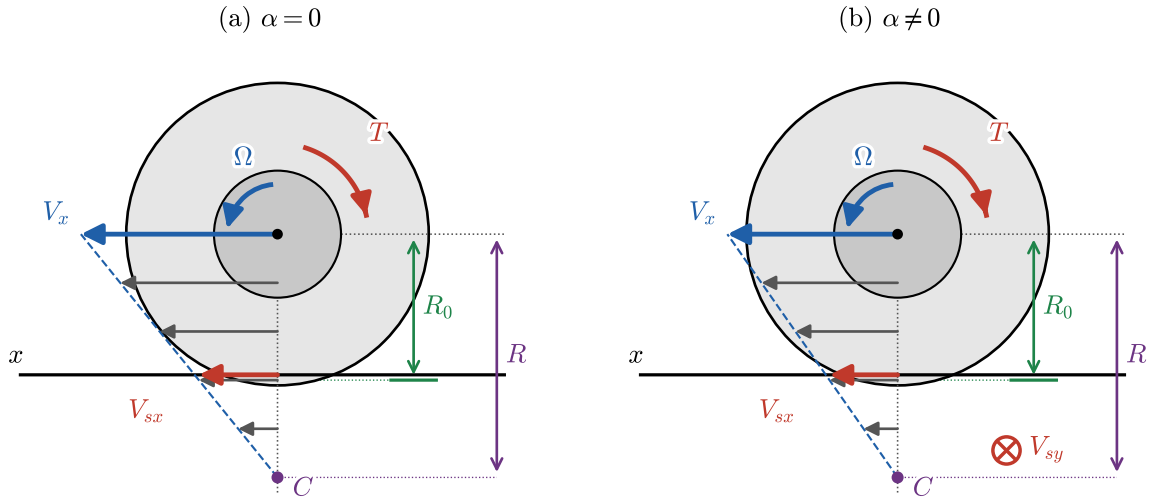


Figure 3.3. Braked wheel, (a) $\alpha = 0$ and (b) $\alpha \neq 0$. Here $\Omega < \Omega_{0\alpha}$, $R > R_0$, C below the road and $V_{sx} > 0$; with $\alpha \neq 0$ also V_{sy}.

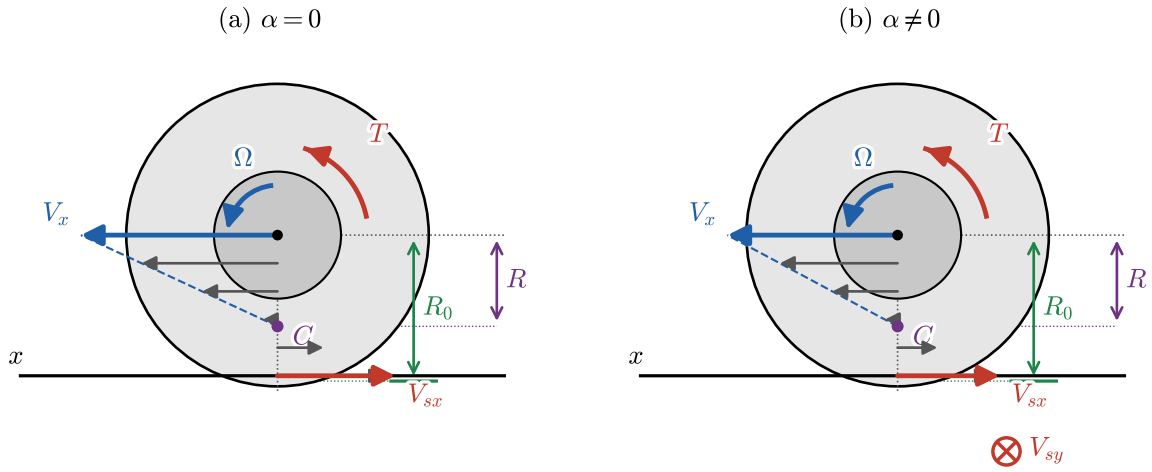


Figure 3.4. Driven wheel, (a) $\alpha = 0$ and (b) $\alpha \neq 0$. Here $\Omega > \Omega_{0\alpha}$, $R < R_0$, C above C_0 and $V_{sx} < 0$; with $\alpha \neq 0$ also V_{sy}.

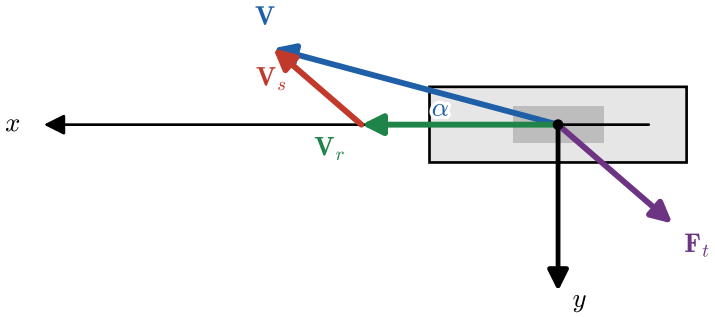
3.4 Slip velocity

The velocity of the wheel center is split into the rolling velocity $\mathbf{V}_r$, the velocity the rim would have if it only rolled at Ω, and the slip velocity $\mathbf{V}_s$, the velocity at which the contact point slides on the road, Figure 3.5.

$$\mathbf{V} = \mathbf{V}_r + \mathbf{V}_s, \qquad \mathbf{V}_r = (\Omega R_0,\ 0), \qquad V_{sx} = V_x - \Omega R_0 = (R - R_0)\,\Omega, \qquad V_{sy} = V_y \tag{3.5}$$

The tire force depends only on $\mathbf{V}_s$, Section 4. $\mathbf{V}_s$ is defined for every motion, whether forward, backward, locked, sideways or at rest.

(a) braked, $\Omega R_0 < V_x$



(b) driven, $\Omega R_0 > V_x$

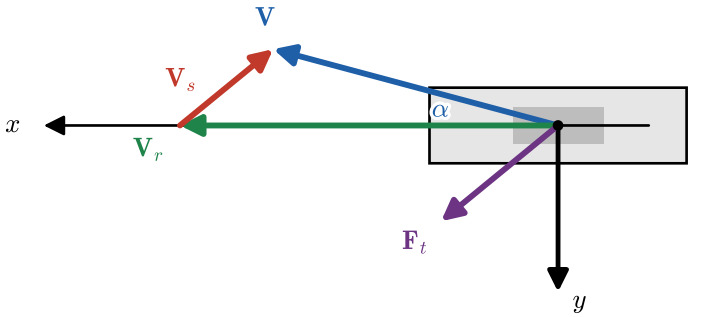


Figure 3.5. Slip velocity at the same slip angle. (a) Braked with $\Omega R_0 < V_x$, the contact point slides forward and $\mathbf{F}_t$ points backward. (b) Driven with $\Omega R_0 > V_x$, it slides backward and $\mathbf{F}_t$ points forward. In both, $\mathbf{F}_t$ is opposite to $\mathbf{V}_s$ and $F_y > 0$.

3.5 Slip indices

The tire force depends on how fast the contact point slides compared with how fast the wheel moves; 1 m/s of sliding is large at 5 m/s and small at 50 m/s. The slip velocity is therefore divided by a reference speed, and the two natural choices give two slip indices [1]. The *practical slip* divides by the speed of the center along the wheel, V_x; the *theoretical slip* divides by the rolling speed of the rim, ΩR_0, at which the tread passes through the patch.

$$\mathbf{s} = \frac{\mathbf{V}_s}{V_x}, \qquad s_x = 1 - \frac{\Omega}{\Omega_{0\alpha}}, \qquad s_y = -\tan\alpha \tag{3.6}$$

$$\boldsymbol{\sigma} = \frac{\mathbf{V}_s}{\Omega R_0}, \qquad \sigma_x = \frac{\Omega_{0\alpha}}{\Omega} - 1, \qquad \sigma_y = -\frac{\Omega_{0\alpha}}{\Omega}\tan\alpha \tag{3.7}$$

Both are $\mathbf{V}_s$ divided by a speed, so they point the same way and are related by

$$\boldsymbol{\sigma} = \frac{\mathbf{s}}{1 - s_x}, \qquad \mathbf{s} = \frac{\boldsymbol{\sigma}}{1 + \sigma_x} \tag{3.8}$$

They are almost equal at small slip and differ near locking and wheel spin, Table 3.2 and Figure 3.6. Both are positive when braking; PAC2002 uses $\kappa = -s_x$ [3]. The same formulas hold for a wheel rolling backward, $V_x < 0$ and $\Omega < 0$, where $s_x > 0$ still means braking.

Condition	Spin	s_x	σ_x
free rolling	$\Omega = \Omega_{0\alpha}$	0	0
braked	$0 < \Omega < \Omega_{0\alpha}$	0 to 1	positive
locked	$\Omega = 0$	1	$+\infty$
driven	$\Omega > \Omega_{0\alpha}$	negative	-1 to 0
spinning	$\Omega \gg \Omega_{0\alpha}$	$\to -\infty$	$\to -1$

Table 3.2. Longitudinal slip in the main rolling conditions.

Each index fails in one condition, $\mathbf{s}$ at $V_x = 0$ for a wheel sliding sideways or spinning in place, and $\boldsymbol{\sigma}$ at $\Omega = 0$ for a locked wheel. The tire law uses only the size of the index, and its force tends to the finite sliding friction $\mu_1 F_z$ as the slip grows, Section 4.2; the transient tire of Section 6 removes the division by the speed altogether. The choice of index for the characteristic is made in Section 4.3.

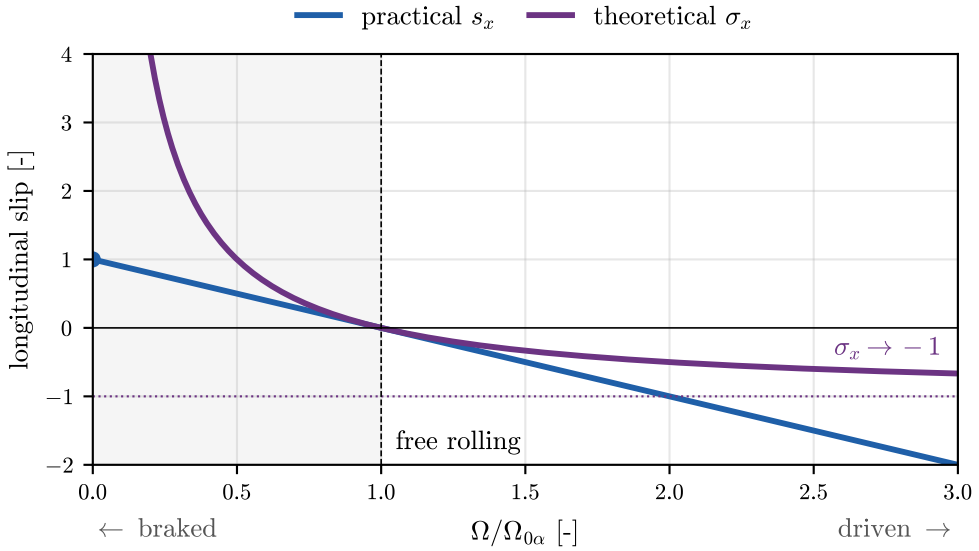


Figure 3.6. Longitudinal slip against the spin, from locked at $\Omega = 0$ through free rolling at $\Omega = \Omega_{0\alpha}$ to driven. The practical slip s_x is finite when locked and grows without limit in wheel spin; the theoretical slip σ_x is infinite when locked and tends to -1 in wheel spin.

4 Tire model

This section gives the tire law, that is the tangential force $\mathbf{F}_t = (F_x, F_y)$ of the road on the tire for a given slip. It gives first its direction, then its size, and finally the two moments the model keeps, rolling resistance and aligning moment.

4.1 Direction of the force on an isotropic tire

By A6 the tire grips the same in every direction. The force is then opposite to the sliding, as in dry friction, and its size depends only on how much the tire slides, through one curve [1]. A. De Felice writes it with the theoretical slip,

$$\mathbf{F}_t = -\frac{\boldsymbol{\sigma}}{\sigma} F_t(\sigma), \qquad \sigma = \|\boldsymbol{\sigma}\| \tag{4.1}$$

The model takes the direction from $\mathbf{V}_s$ itself. Both slip indices are $\mathbf{V}_s$ divided by a speed, so they point the wrong way when that speed is negative, for a wheel rolling backward, and are infinite when it is zero. $\mathbf{V}_s$ is always the true direction of sliding, and using it is a design choice.

$$\mathbf{F}_t = -\frac{\mathbf{V}_s}{\|\mathbf{V}_s\|} F_t \tag{4.2}$$

This single formula covers pure slip, braking, driving, combined slip, the locked wheel, where $\mathbf{F}_t$ points against $\mathbf{V}$, and the wheel sliding sideways at any α. No special rule is needed above 90°. As a sign check, in pure slip with $\alpha > 0$, $\mathbf{V}_s = (0, -V \sin\alpha)$ points to the right, so $F_y > 0$; braking forward, $V_{sx} > 0$, so $F_x < 0$; in free rolling straight ahead $\mathbf{V}_s = 0$ and there is no force.

A real tire is not isotropic. At small slip it has a longitudinal slip stiffness C_x and a cornering stiffness C_α, the force per unit slip along x and along y, in general different. For a slip of size σ at an angle θ from x, the force per unit slip is

$$C(\theta) = \sqrt{(C_x \cos\theta)^2 + (C_\alpha \sin\theta)^2} \tag{4.3}$$

which describes an ellipse over all directions, Figure 4.1, and the force does not point exactly against the slip. The isotropic tire takes $C_x = C_\alpha = C_s$, so the ellipse becomes a circle of radius C_s, the slip stiffness, and the force is exactly opposite to the slip.

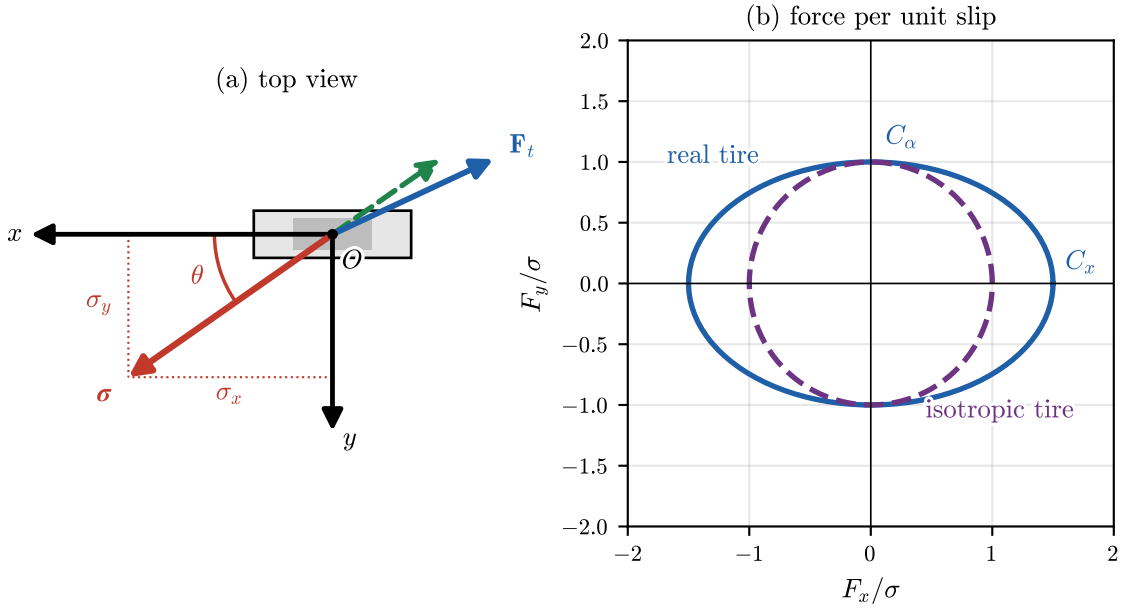


Figure 4.1. Slip stiffness, with illustrative values $C_x = 1.5$ and $C_\alpha = 1$. (a) Top view, with the slip $\boldsymbol{\sigma}$ at angle θ from x and the force per unit slip, solid for a real tire and dashed for the isotropic tire. (b) The force per unit slip over all slip directions, an ellipse for a real tire and a circle of radius $C_s = C_\alpha$ for the isotropic tire.

4.2 Characteristic

The size of the force against the size of the slip is linear at small slip, $F_t \approx C_s\sigma$. It reaches a peak $\mu_0 F_z$ at the slip σ_p, when a growing part of the patch slides, and tends to the sliding friction $\mu_1 F_z < \mu_0 F_z$ as the slip grows without limit. The curve is the Magic Formula [3], written here as A. De Felice writes it, in the theoretical slip [1]; which slip index the model feeds to it is decided in Section 4.3.

$$F_t(\sigma) = D\sin(C\arctan(B\sigma - E(B\sigma - \arctan B\sigma))) \tag{4.4}$$

$D = \mu_0 F_z$ is the peak; C is the shape factor, with $F_t(\infty) = D\sin(C\pi/2) = \mu_1 F_z$ for $E < 1$; E is the curvature near the peak; B is the stiffness factor, with $BCD = C_s$. On the isotropic tire one curve and one friction coefficient describe every direction. The model uses the PAC2002 lateral coefficients, so $C_s = C_\alpha$, and the longitudinal stiffness, peak and slip at the peak are taken equal to the lateral ones (limitation L2). The factors follow from the tire file and the load, Section 4.5.

4.3 Practical slip in the characteristic

Equation (4.4) is written in the theoretical slip σ. The model feeds the practical slip instead, with the same coefficients.

$$F_t(s) = D\sin(C\arctan(Bs - E(Bs - \arctan Bs))), \qquad s = \|\mathbf{s}\| = \sqrt{s_x^2 + s_y^2} \tag{4.5}$$

There are two reasons. First, PAC2002 is written in practical slip. Its inputs are the longitudinal slip $\kappa = -s_x$ and $\tan\alpha = -s_y$, both $\mathbf{V}_s$ divided by $|V_x|$, and the coefficients of the tire file are fitted to measured force against these [3]. In pure lateral slip $s = |\tan\alpha|$, exactly the input of the file. Second, the transient tire of Section 6 gives practical slip, because in steady state its transient slip becomes $\mathbf{V}_s/|V_x| = \mathbf{s}$, not $\boldsymbol{\sigma}$.

Figure 4.2 draws this curve at the reference load. The peak is at s_p, and the force tends to $\mu_1 F_z$ as $s \to \infty$, for a wheel spinning without limit or sliding sideways with $V_x = 0$. A locked wheel has the finite slip $s = 1/|\cos\alpha|$, so its force is $F_t(s = 1) = 0.996\,F_z$ at $\alpha = 0$ and not $\mu_1 F_z$, the value that Equation (4.4) would give with σ, which is infinite there.

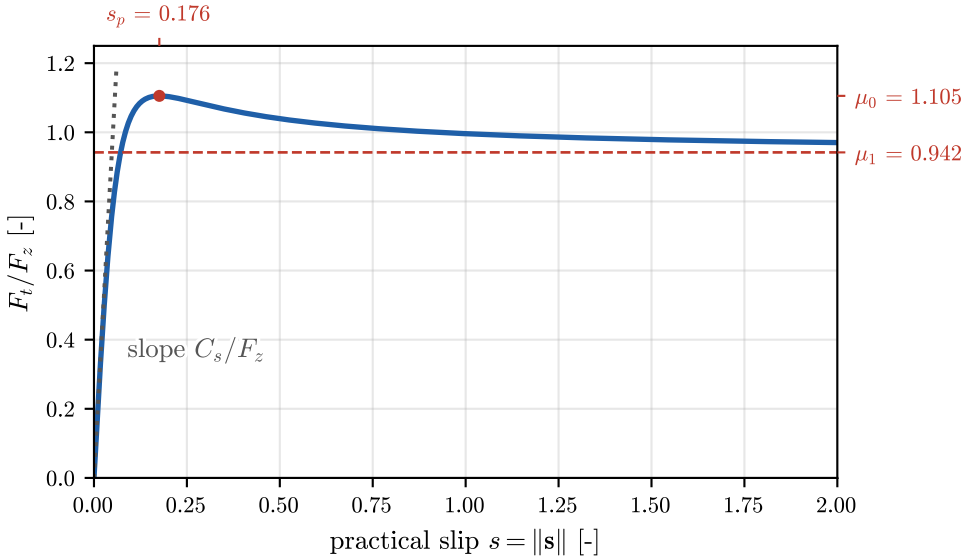


Figure 4.2. Characteristic with the lateral coefficients of the tire file at the reference load $F_z = 2.70$ kN, against the practical slip, with the linear part of slope C_s, the peak μ_0 at s_p and the sliding limit μ_1.

The same tire can be written in σ. With $\mathbf{s} = \boldsymbol{\sigma}/(1 + \sigma_x)$ from Equation (3.8),

$$F_\sigma(\boldsymbol{\sigma}) = F_t\Big(\frac{\|\boldsymbol{\sigma}\|}{1 + \sigma_x}\Big) \tag{4.6}$$

gives the same force as $F_t(s)$ at every slip, by construction. Written in σ, the curve depends on the direction of the slip through σ_x, Figure 4.3. It is F_t itself in pure lateral slip, is stretched when braking, tending to $0.996\,F_z$ as the wheel locks, and is compressed when driving, reaching $\mu_1 F_z$ at $\|\boldsymbol{\sigma}\| = 1$. The model uses the curve in s; this form only links it to the notation of A. De Felice [1].

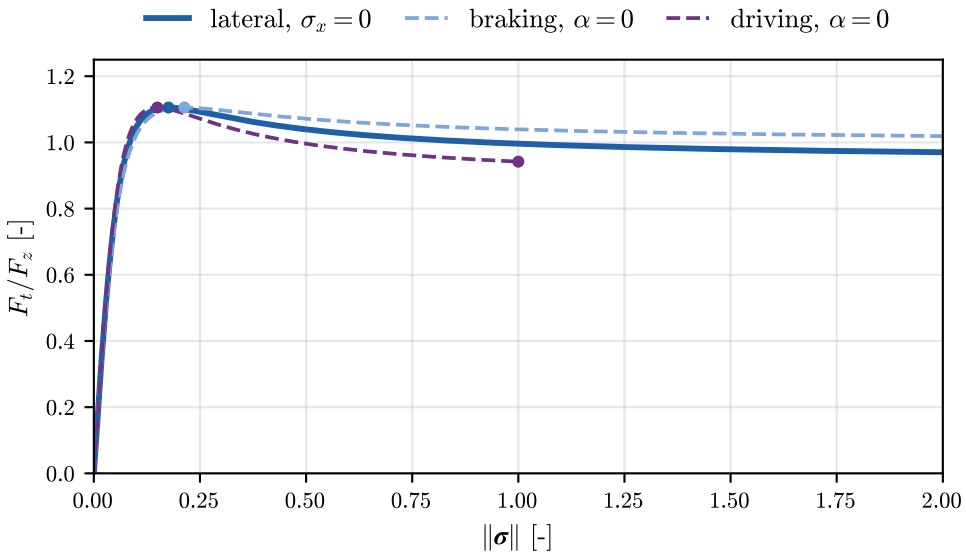


Figure 4.3. The tire of the model written in the theoretical slip, Equation (4.6), at the reference load $F_z = 2.70$ kN. Solid, pure lateral slip, the curve of Figure 4.2 against σ; thin dashed, braking and driving at $\alpha = 0$, the two limits. The dots mark the peaks and the end of the driving curve at μ_1.

4.4 Combined slip

The polar diagrams of Figures 4.4 and 4.5 show F_x and F_y of the model, Equation (4.2) with Equation (4.5), when both slips are present. In Figure 4.4 the slip angle is fixed and the spin is swept from wheel spin, through free rolling, to locked. Each curve starts on the driven side, on the circle $\mu_1 F_z$ of a wheel spinning without limit, crosses pure slip where $F_x = 0$ and ends at the locked wheel with $F_t(s = 1/\cos\alpha)$, between the circles $\mu_1 F_z$ and $\mu_0 F_z$ and $0.996\,F_z$ at small α; the diagram shows how braking or driving reduces the lateral force at a given slip angle.

In Figure 4.5 the lateral slip σ_y is fixed and σ_x is swept along the whole axis. A wheel rolling forward reaches only $\sigma_x > -1$; values below -1 need V_x and Ω of opposite sign, which the rig reaches with the wheel turned past 90° and driven against its motion, scenario S9 of Section 8. No curve leaves the circle $\mu_0 F_z$, the friction circle, because the isotropic tire has one peak for the size of the force in every direction.

4.5 Pure slip and load

In pure lateral slip $V_{sx} = 0$ and $s_y = -\tan\alpha$, so the slip size is $s = |\tan\alpha|$ and Equation (4.5) gives the lateral force directly.

$$F_y(\alpha) = F_t(\tan\alpha), \qquad 0 \le \alpha < 90° \tag{4.7}$$

In pure longitudinal slip at $\alpha = 0$ the same curve gives $|F_x| = F_t(|s_x|)$. The longitudinal curve $F_x(s_x)$ and the lateral curve $F_y(\alpha)$ are therefore one curve read against two abscissae, s and $\alpha = \arctan s$. They have the same slope at the origin, $C_x = C_\alpha = C_s$, and the same peak, reached at s_p along x and at $\alpha_p = \arctan s_p$, 10.0° at the reference load. The angle compresses

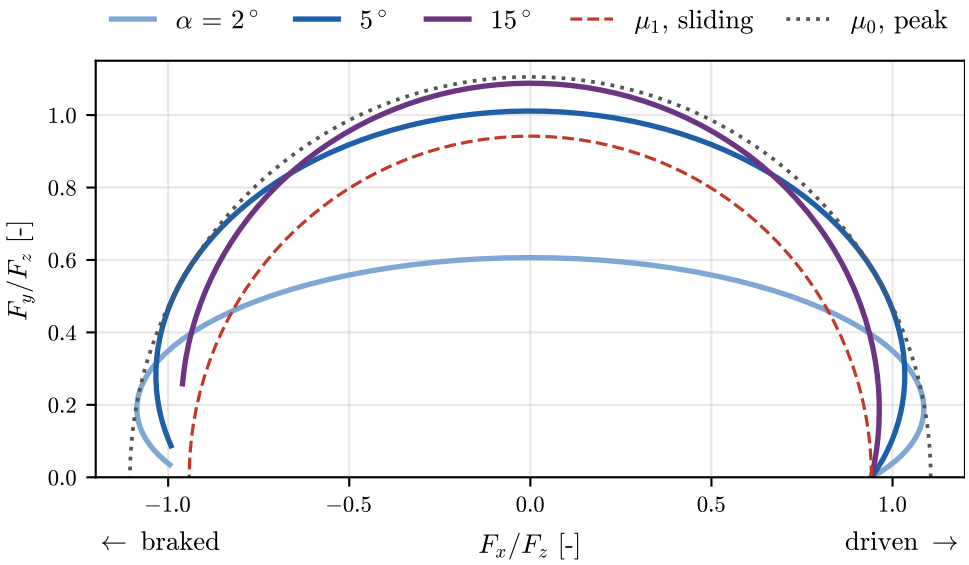


Figure 4.4. Polar diagram at constant slip angle, at the reference load. $(F_x, F_y)/F_z$ for each α, with the spin swept from wheel spin on the right to locked on the left.

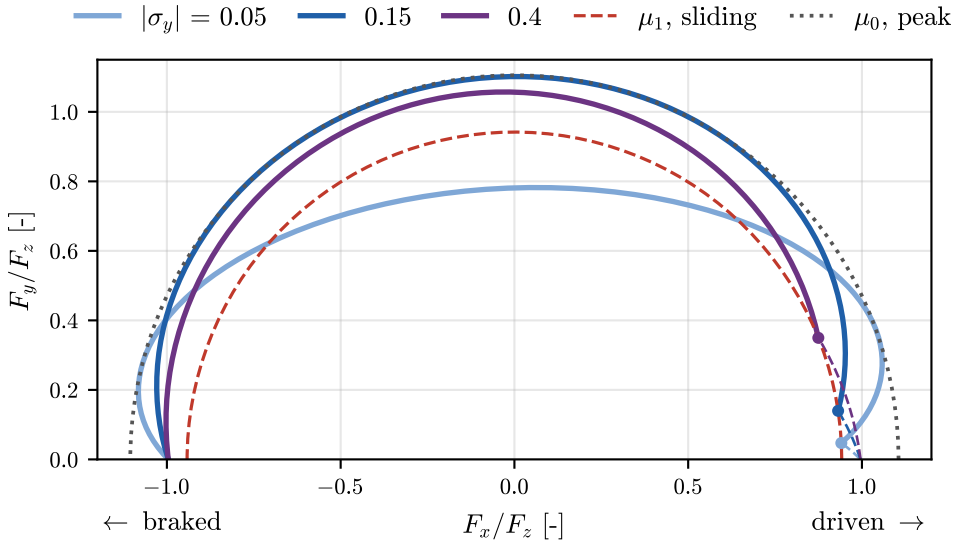


Figure 4.5. Polar diagram at constant lateral slip, at the reference load. $(F_x, F_y)/F_z$ for each $|\sigma_y|$, with σ_x swept along the whole axis. From the left end to the dot, $\sigma_x > -1$ and $\delta < 90°$; at the dot, $\sigma_x = -1$ and $\delta = 90°$; beyond it, dashed, $\sigma_x < -1$ and $\delta > 90°$, the wheel driven against its motion, from spinning in place at the dot, on the circle $\mu_1 F_z$, to a locked wheel sliding backward, $0.996\,F_z$ on the F_x axis.

large slips. A locked wheel, $s_x = 1$, matches $\alpha = 45°$, and the sliding limit $\mu_1 F_z$, $s \to \infty$, matches $\alpha \to 90°$. In a real tire the two curves differ; the model takes them equal by A6 (limitation L2).

The factors of the characteristic depend on the contact load through the lateral coefficients of the tire file [3],

$$\mu_0 = p_{Dy1} + p_{Dy2}\,df_z, \qquad E = p_{Ey1} + p_{Ey2}\,df_z \le 1, \qquad df_z = \frac{F_z - F_{z0}}{F_{z0}}$$
$$C_s = p_{Ky1} F_{z0} \sin\!\left(2 \arctan \frac{F_z}{p_{Ky2} F_{z0}}\right) \tag{4.8}$$

with $D = \mu_0 F_z$, $C = p_{Cy1}$ and $B = C_s/(CD)$, so that $BCD = C_s$ as in Equation (4.4). Table 4.1 gives the coefficients and the factors at the reference load, where $df_z = -0.313$.

The peak friction falls as the load grows and the slip stiffness grows less than the load, Figure 4.6. Between $0.5F_{z0}$ and $1.5F_{z0}$, μ_0 falls from 1.14 to 0.96, C_s/F_z from 20.6 to 14.0, and the peak moves from $\alpha_p = 9.8°$ to 12.0°. At every slip angle the lateral force therefore grows less than in proportion to the load; at 15° it is close to the peak $\mu_0 F_z$ and follows the falling friction coefficient, Figure 4.6b. Figure 4.7 shows the whole function $F_y(\alpha, F_z)$ in the load range of the rig. The curves away from the reference load use the load terms of the file, which does not state the loads it was fitted on, Section 2.4.

Factor	Coefficients	Values	At the reference load
μ_0	p_{Dy1}, p_{Dy2}	1.049, −0.180	1.105
C	p_{Cy1}	1.351	1.351
E	p_{Ey1}, p_{Ey2}	−0.00747, −0.00632	−0.00549
C_s	p_{Ky1}, p_{Ky2}	21.92, 2.001	52.9 kN
B	$C_s/(CD)$	–	13.1

Table 4.1. Lateral coefficients from the tire file and factors at the reference load $F_z = 2.70$ kN.

4.6 Rolling resistance

The rubber returns less energy than it stores, so the contact pressure is higher at the front of the patch and its resultant F_z acts a distance e ahead of O, Figure 4.8. About the axle this gives a moment against the rotation [1]

$$M_y = -\nu f F_z h, \qquad f = \frac{e}{h} \tag{4.9}$$

where $\nu = \text{sign}(\Omega)$ while the wheel rolls; at rest the moment becomes part of the friction torque that holds the wheel, Section 5.4. The rolling-resistance coefficient f replaces a pressure distribution that the model does not compute with one number. In free rolling the wheel balances M_y with $F_x = -f F_z$. At constant V the load cell reads this drag, which the belt drive overcomes.

The coefficient grows with the rolling speed ΩR_0 and not with V_x, because the losses come from the tread rolling through the patch.

$$f = f_0 + K_f \, (\Omega R_0)^2, \qquad f_0 = 0.015, \qquad K_f = 5.2 \cdot 10^{-7} \text{ s}^2/\text{m}^2 \tag{4.10}$$

In free rolling $\Omega R_0 = V_x$, the form given by A. De Felice [1]. f_0 is his value on asphalt; K_f is the radial-ply value of J. Y. Wong [4], quoted and not yet checked against the source. f is 0.0152 at 20 m/s and 0.0169 at 60 m/s, Figure 4.9, so it is almost constant in the range of the rig. The steep rise above the critical speed of the tire is not represented (limitation L3). Rolling resistance can be switched off; in the spin equation it is a friction torque added to the brake, Section 5.4.

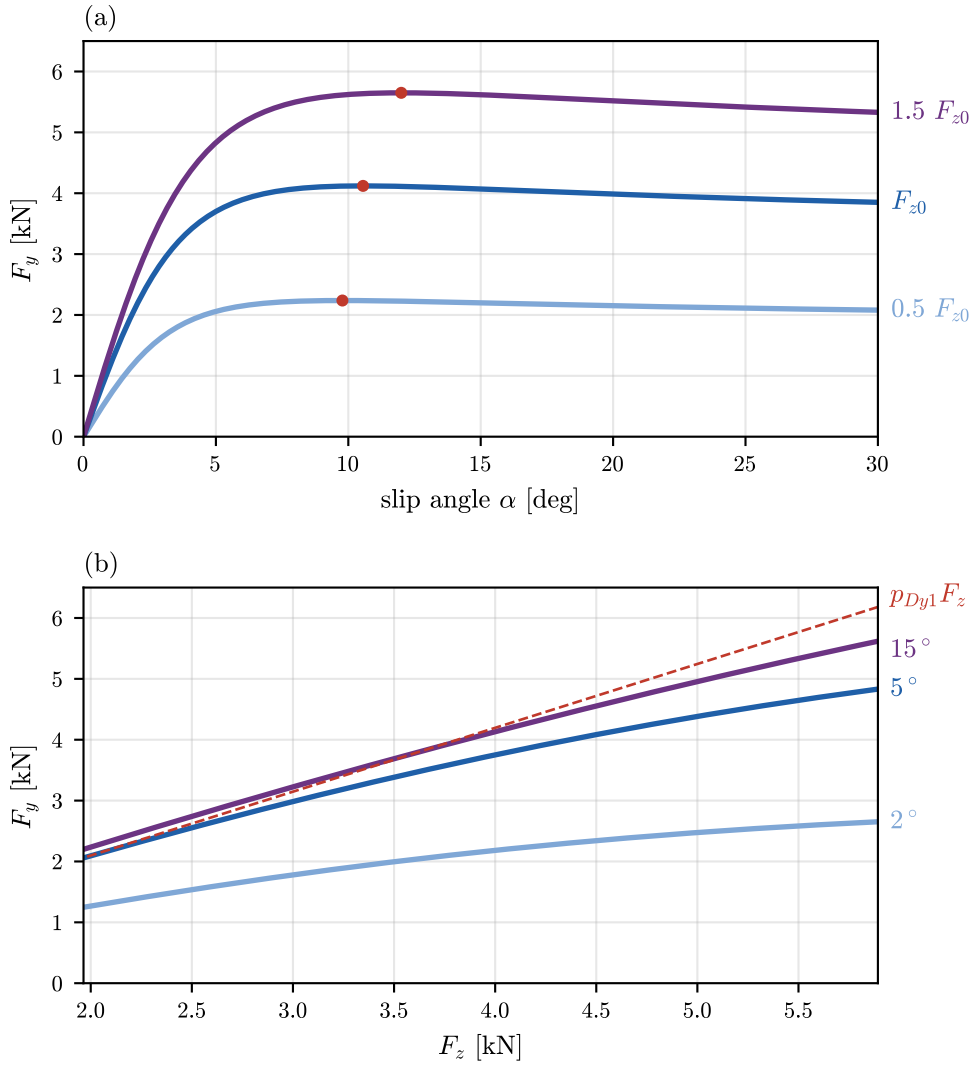


Figure 4.6. Lateral force in pure slip, Equations (4.7) and (4.8). (a) Against the slip angle at $0.5F_{z0}$, F_{z0} and $1.5F_{z0}$; the dots mark the peaks $\mu_0 F_z$ at α_p. (b) Against the load at three slip angles, with, dashed, the line $p_{Dy1}F_z$ of a friction coefficient independent of the load.

4.7 Aligning moment

The lateral force acts a distance t, the *pneumatic trail*, behind O, because the tread is deflected more and more from the front to the rear of the patch. About z it gives the moment

$$M_z = -t\, F_y \tag{4.11}$$

The moment turns the wheel toward **V**, hence its name, Figure 4.10. On the rig δ is imposed, so M_z does not change the motion and appears only in the steering moment at the hub, Equation (5.4).

Only F_y has a trail; F_x would add to M_z only through a lateral offset of the patch, which the model leaves out (limitation L4).

The lateral deflection of the tread grows from the front of the patch, where the tread enters undeformed, toward the rear, so the lateral stress is larger toward the rear and its resultant F_y acts behind the center of the patch, Figure 4.10. As α grows the rear of the patch starts to slide and the trail falls.

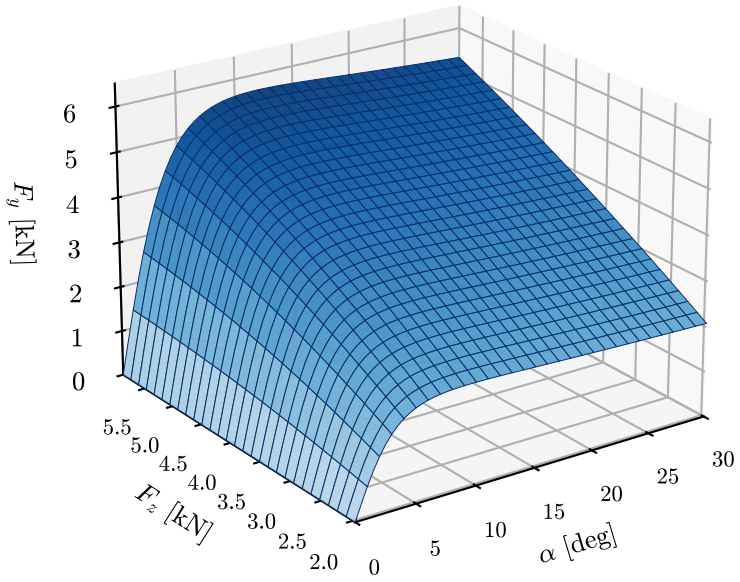


Figure 4.7. Lateral force in pure slip against slip angle and load, over the load range of the rig.

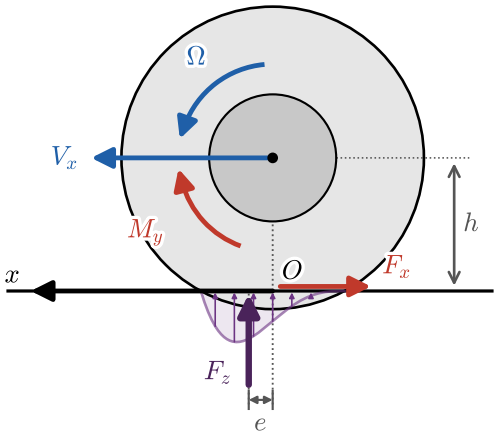


Figure 4.8. Rolling resistance, side view, offset exaggerated. The contact pressure is higher at the front, so its resultant F_z acts at e ahead of O and gives the moment M_y against Ω. In free rolling the road force $F_x = -fF_z$ balances it, with $f = e/h$.

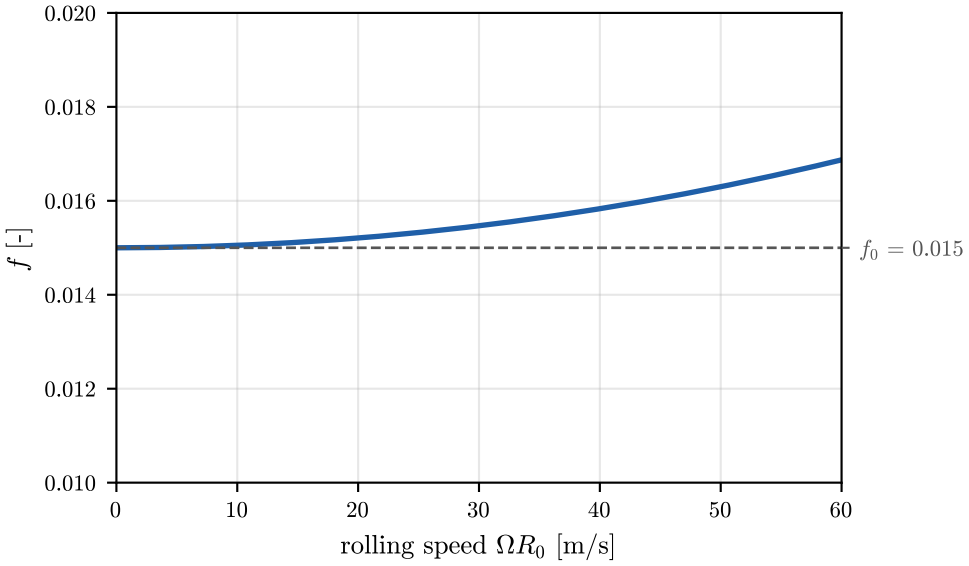


Figure 4.9. Rolling-resistance coefficient $f = f_0 + K_f(\Omega R_0)^2$ against the rolling speed.

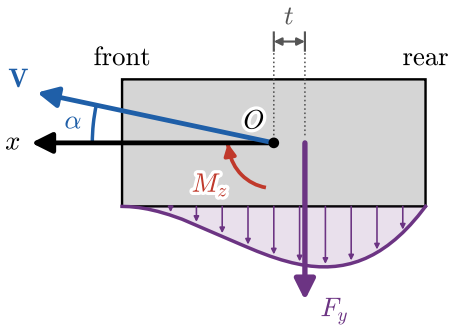


Figure 4.10. Contact patch in top view at $\alpha = 3°$ and the reference load. $F_y = 2.17$ kN from Equation (4.5) acts the trail $t = 16.7$ mm behind O, from Equations (4.12) to (4.14), so that $M_z = -tF_y = -36$ N m turns the wheel toward **V**. Lateral stress along the patch illustrative. Patch half-length estimated as $\sqrt{2R_e\rho} = 81$ mm with the deflection ρ of Section 5.1, width schematic, slip angle drawn enlarged.

PAC2002 describes the trail with a cosine Magic Formula, here at zero camber [3].

$$t = D_t \cos\Big(C_t \arctan\left(B_t\alpha_t - E_t\left(B_t\alpha_t - \arctan B_t\alpha_t\right)\right)\Big)\cos\alpha, \qquad \alpha_t = |\tan\alpha| \tag{4.12}$$

$$D_t = F_z\left(q_{Dz1} + q_{Dz2}\,df_z\right)\frac{R_e}{F_{z0}}, \qquad B_t = q_{Bz1} + q_{Bz2}\,df_z + q_{Bz3}\,df_z^2, \qquad C_t = q_{Cz1} \tag{4.13}$$

$$E_t = \left(q_{Ez1} + q_{Ez2}\,df_z\right)\Big(1 + q_{Ez4}\,\tfrac{2}{\pi}\arctan(B_tC_t\,\alpha_t)\Big) \le 1 \tag{4.14}$$

D_t is the trail at zero slip; B_t, C_t and E_t shape its fall, as B, C and E do in Equation (4.4); df_z is the load change of Equation (4.8) and α_t is the slip input of the trail, discussed below. Table 4.2 gives the coefficients from the tire file and the resulting factors at the reference load.

Factor	Coefficients	Values	At the reference load
D_t	q_{Dz1}, q_{Dz2}	0.0935, −0.00922	22.8 mm
B_t	q_{Bz1}, q_{Bz2}, q_{Bz3}	10.90, −1.841, −0.520	11.4
C_t	q_{Cz1}	1.214	1.214
E_t	q_{Ez1}, q_{Ez2}, q_{Ez4}	−1.570, 0.334, 0.267	−1.67 at $\alpha = 0$

Table 4.2. Trail coefficients from the tire file and factors at the reference load $F_z = 2.70$ kN.

At the reference load, between the lower two curves of Figure 4.11, the trail falls from 22.8 mm to zero at $\alpha = 9.5°$, about where F_y peaks. M_z therefore peaks early, at −36 N m for $\alpha = 2.9°$, and has almost vanished at the force peak, so the steering goes light before the limit. The trail at zero slip grows with the load, as D_t in Equation (4.13), and so does the peak of M_z, −20, −70 and −136 N m at $0.5F_{z0}$, F_{z0} and $1.5F_{z0}$.

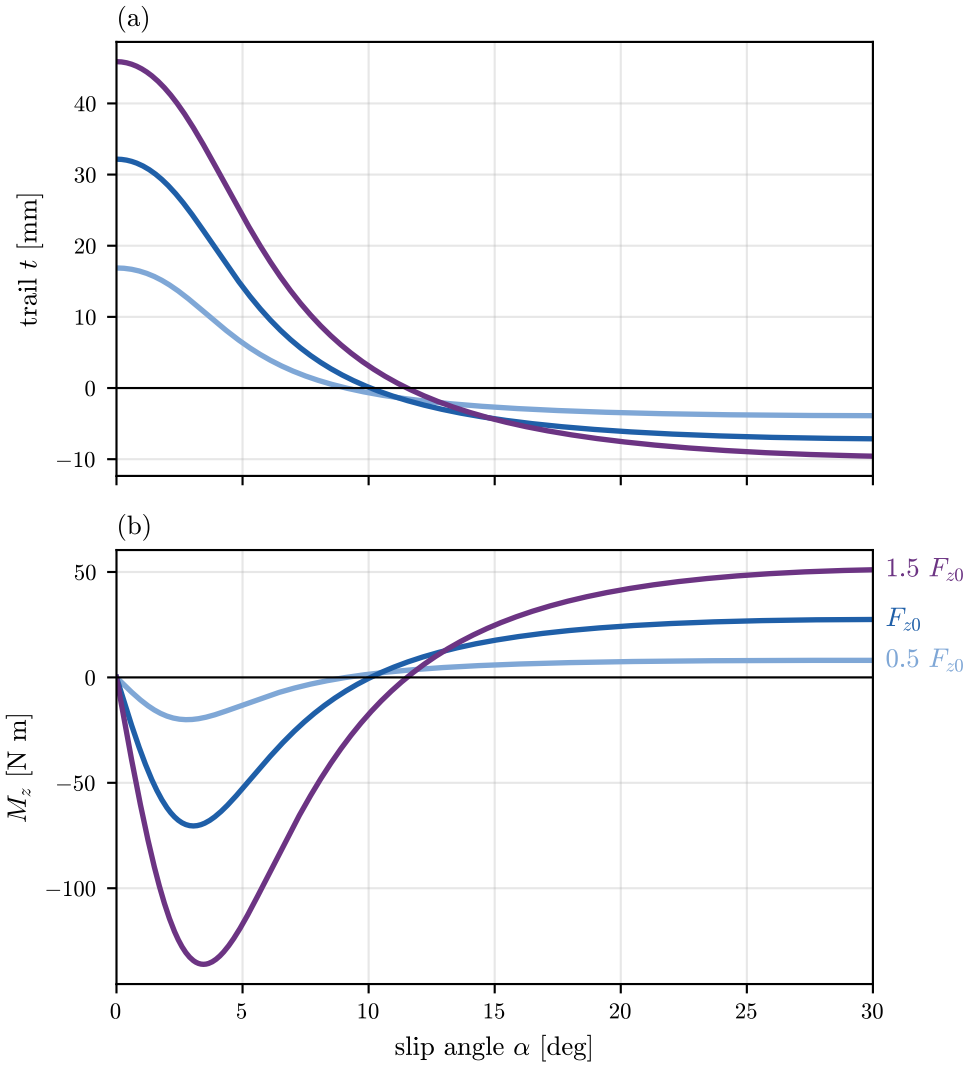


Figure 4.11. Pure slip at $0.5F_{z0}$, F_{z0} and $1.5F_{z0}$, named in (b), with the colors of Figure 4.6. (a) Pneumatic trail t against the slip angle. (b) Aligning moment $M_z = -tF_y$.

Three choices complete the aligning moment. In combined slip $M_z = -t(\alpha)\, F_y$, with F_y from Equation (4.2), which is the default of Chrono [2]; the full combined law of H. B. Pacejka also uses the longitudinal slip in the trail and adds a moment of F_x, but the file has no coefficients for it (limitation L4). The horizontal shift and the residual torque of PAC2002 are left out, because

both make the tire asymmetric and a wheel rolling straight would feel a steering torque; then $M_z = 0$ at $\alpha = 0$. Finally, PAC2002 feeds the trail with $\tan\alpha$, as the lateral force [3], and is fitted for $|\alpha| < 90°$. The curve therefore takes $\alpha_t = |\tan\alpha|$, which is the same for a wheel rolling forward or backward at the same angle between wheel plane and $\mathbf{V}$; the factor $\cos\alpha$ makes t vanish at 90° and change sign beyond, so that the trail of a wheel rolling backward stays behind it relative to the motion. This extension is a hypothesis, outside the fitted range of the file (limitation L5). At $V = 0$, where α is undefined, the trail is taken at $\alpha = 0$, its value without sliding, a design choice.

5 Wheel dynamics

The system is the wheel, rim and tire together. The frame enters only through the actions it applies at the hub H, the center of the axle at the height h above O. This section writes the balance of the wheel, gives the hub actions and derives the spin equation.

5.1 Masses, load and radii

The masses and loads are those of Table 2.2. The wheel is the Chrono sedan wheel [2]; the reference load on the fork is chosen so that the contact load $F_z = P + m_w g$, Equation (5.2), is a quarter of the weight of an 1100 kg car.

At this load the tire law gives $C_s = 52.9$ kN and $\mu_0 = 1.105$, Table 4.1. The tire figures of Section 4 are drawn at this load, except Figures 4.6, 4.7 and 4.11, which span the load range.

The radii are fixed (A4), computed once at the reference load from the unloaded radius $R_e = 0.344$ m and the vertical stiffness $c_z = 281$ kN/m of the tire file. The deflection is $\rho = F_z/c_z = 9.6$ mm. The loaded radius h, height of the hub and lever arm of F_x, is R_e minus the whole deflection. The free-rolling radius R_0 lies a third of the way down, because the steel belt of the tire hardly stretches; this is also the estimate used by Chrono [2].

$$h = R_e - \rho = 0.334 \text{ m}, \qquad R_0 = R_e - \frac{\rho}{3} = 0.341 \text{ m} \tag{5.1}$$

The radii are not recomputed when the load changes. At the ends of the load range the same formulas give R_0 within 1.1 % and h within 3.5 % of the fixed values, the largest errors at $1.5F_{z0}$. The error on R_0 shifts the free-rolling spin by the same fraction; the error on h changes the lever of F_x and so the locking torque (limitation L13).

5.2 Free-body diagram and balance

Figure 5.1 shows every action on the wheel, drawn with $\delta = 0$ in its positive direction; forces are straight arrows and moments curved arrows by the right-hand rule. The road acts at O with the forces F_x, F_y, F_z and the moments M_x, M_y, M_z, all from the tire law except F_z, which follows from the balance, and $M_x = 0$ by A5. The weight $m_w g$ acts at H. The frame acts at H through the fork with the forces R_{hx}, R_{hy} and $R_{hz} = -P$, the vertical load, and with the moments M_{hx} and M_{hz}; it applies no moment about the axle. The torque T of the motor or brake on the fork acts about the axle, Section 5.4.

The hub is held by the frame and does not accelerate. The belt moves, not the wheel, which only spins at Ω about y. The steering inertia and the gyroscopic moment $J_w\Omega\dot{\delta}$ are neglected, A7. They only load the hub and never change Ω or the forces. At 20 m/s and the steer rate of 60°/s the gyroscopic moment is about 7 % of the largest hF_y, an estimate. They return in the simulator, where the wheel carrier rolls, pitches and steers (limitation L6).

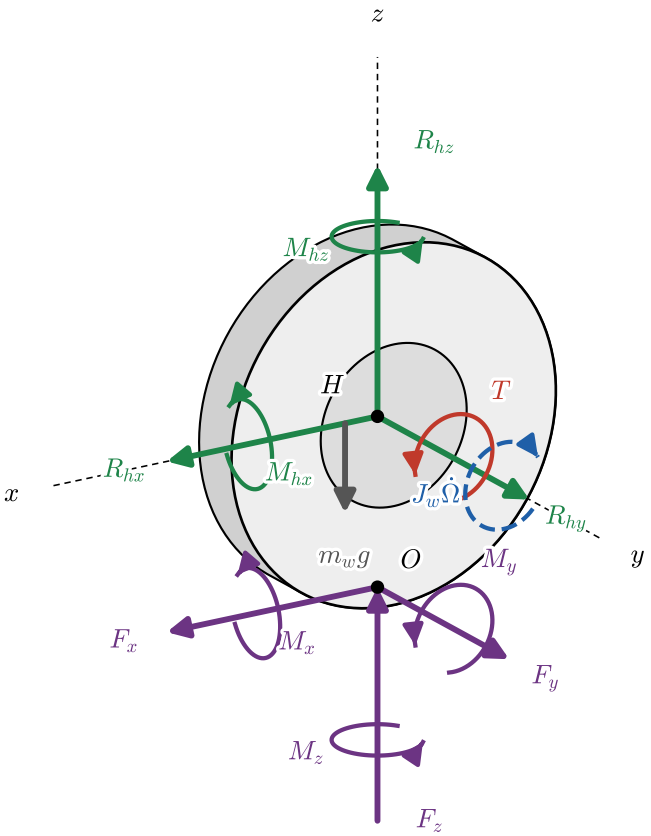


Figure 5.1. Free-body diagram of the wheel. The road acts on the tire at O with the forces F_x, F_y, F_z and the moments M_x, overturning, M_y, rolling resistance, and M_z, aligning. The frame acts on the wheel at the hub H with the forces R_{hx}, R_{hy} and $R_{hz} = -P$ and the moments M_{hx}, M_{hz}, none about the axle. Torque T from the motor or brake on the fork, weight $m_w g$ at H; dashed, the inertia moment $J_w\dot{\Omega}$.

With the road forces applied at $-h\,\mathbf{e}_z$ from H, the balance of forces and of moments about H reads

$$0 = F_x + R_{hx}, \qquad 0 = F_y + R_{hy}, \qquad 0 = F_z - P - m_w g \tag{5.2}$$

$$0 = M_{hx} + hF_y + M_x, \qquad J_w\dot{\Omega} = T - hF_x + M_y, \qquad 0 = M_{hz} + M_z \tag{5.3}$$

The vertical balance gives the contact load $F_z = P + m_w g$. The moment about the axle is the spin equation of Section 5.4.

5.3 Hub actions

The remaining equations give the hub actions.

$$R_{hx} = -F_x, \qquad R_{hy} = -F_y, \qquad R_{hz} = -P, \qquad M_{hx} = -hF_y - M_x, \qquad M_{hz} = -M_z \tag{5.4}$$

The hub reads the tire forces directly, which is what the load cell of a real machine measures. M_{hx} is the moment of F_y about the hub, and M_{hz} is the steering torque that holds δ. In the simulator these actions, reversed, will be the loads on the chassis.

The tire force can also be split along the belt direction $\mathbf{e}_r$ and across it, along $\mathbf{e}_n = (\sin\delta, \cos\delta)$.

$$F_\parallel = F_x \cos\delta - F_y \sin\delta, \qquad F_\perp = F_x \sin\delta + F_y \cos\delta \tag{5.5}$$

$-F_\parallel V$ is the power the belt drive spends to keep V. With a slip angle and no torque, $F_\parallel = -F_y \sin\delta < 0$. This is the cornering drag, which slows a car in a corner.

5.4 Spin equation and torque inputs

The throttle gives a drive torque $T_D \geq 0$ and the brake pedal a brake torque $T_B \geq 0$; a single signed motor torque would spin the wheel backward at standstill. The brake and the rolling resistance of Equation (4.9) are friction torques. While the wheel rolls they oppose Ω with the size

$$T_f = T_B + f F_z h \tag{5.6}$$

and the net torque on the rim and the spin equation, from Equation (5.3), are

$$T = T_D - \nu T_B, \qquad J_w \dot{\Omega} = T_D - h F_x - \nu T_f, \qquad \nu = \operatorname{sign}(\Omega) \tag{5.7}$$

While the wheel rolls forward the net torque is simply $T_D - T_B$, so both pedals can be pressed at once. T is a couple between the fork, which carries the motor or caliper, and the rim. It has no net force and acts only through the slip. T changes Ω, Ω changes the slip and the slip gives F_x. In the hub balance the brake and the rolling resistance stay apart, because the reaction of T_B goes into the fork while M_y comes from the road. In steady rolling, $\dot{\Omega} = 0$ and $T = h F_x - M_y$. At constant V, each torque below the locking torque T_{lock} of Section 5.5 gives one steady point of the longitudinal characteristic, which is the purpose of the rig.

A friction torque cannot reverse the spin. It can only stop the wheel and hold it, and at $\Omega = 0$ it takes whatever value between $-T_f$ and T_f keeps the wheel at rest, Figure 5.2. The torque it must hold is the rest of the spin equation,

$$T_h = T_D - h F_x \tag{5.8}$$

A wheel at rest therefore obeys

$$\dot{\Omega} = 0 \quad \text{if} \quad |T_h| \leq T_B + f_0 F_z h, \qquad J_w \dot{\Omega} = T_h - \nu T_f \quad \text{with} \quad \nu = \operatorname{sign}(T_h) \quad \text{otherwise} \tag{5.9}$$

In the first case the wheel is held, locked by the brake or at rest on the tire. In the second it breaks free and starts to turn in the direction of T_h. The holding limit is the friction torque at $\Omega = 0$, with $f = f_0$, so that a wheel that breaks free does not stop again at the next instant. A held wheel is recognized from $\Omega = 0$ itself, so the switch needs no state of its own. The same rule, a brake that can lock, is offered by the vehicle brake of Project Chrono [5].

The switch replaces the usual smooth sign, $\tanh(\Omega/\Omega_s)$. A smooth sign lets a locked wheel creep, limits the time step near $\Omega = 0$ and adds a parameter without physical meaning; the switch holds the wheel at exactly $\Omega = 0$ and has none of these costs. Its price is a jump of the friction torque when the wheel locks or breaks free, which matters only to an optimiser that uses gradients. Its treatment within a time step is given in Section 7.2.

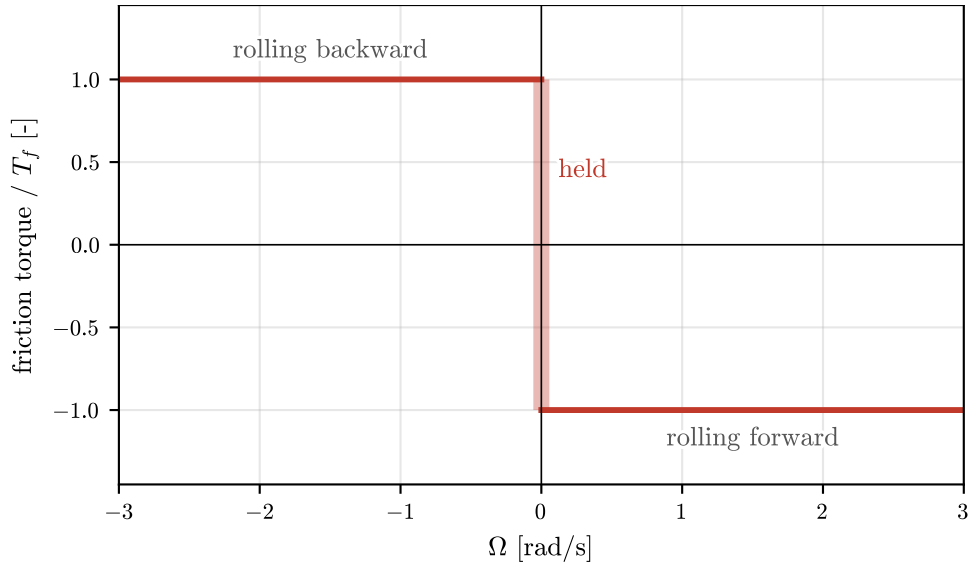


Figure 5.2. Friction torque on the rim divided by T_f, against the spin. While the wheel rolls the torque is $-T_f \operatorname{sign}(\Omega)$. At $\Omega = 0$ it takes any value between $-T_f$ and T_f that holds the wheel, the shaded segment; the wheel breaks free when the torque to be held, T_h, leaves this segment.

5.5 Stability under torque input

The largest torque with a steady point is the locking torque, the torque at the peak force with $\delta = 0$ at constant V, from the steady form of Equation (5.7) with rolling resistance neglected,

$$T_{lock} \approx \mu_0 F_z h \tag{5.10}$$

0.997 kN m at the reference load. Past the peak of F_x no steady point is stable under a torque input. On the falling branch a small increase of slip lowers the tire torque hF_x, so the net torque grows and the slip grows further. A torque above T_{lock} has no steady point at all and the wheel locks or spins. The longitudinal curve is therefore measured up to the peak and at locking; measuring the falling branch would need an imposed spin, which is not planned (limitation L8). The lateral curve $F_y(\alpha)$ is measured whole, by sweeping δ. Scenario S19 of Section 8.2 confirms this.

The same mechanism gives hysteresis. A locked wheel spins up again as soon as the tire torque $-hF_x$, positive because the braking force is $F_x < 0$, exceeds the holding limit of Equation (5.9). The locked tire gives $F_t(s = 1) = 0.996\, F_z$, less than the peak $\mu_0 F_z$, so the wheel releases only at a brake torque below the one that locked it. A spinning wheel recovers in the same way once T_D falls below $\mu_1 F_z h$. The thresholds are given in Table 8.1 and tested by S14. In a vehicle the reaction of T and the moment of F_x also pitch the body and change F_z, dive and squat (limitation L9).

6 Transient tire

6.1 Purpose

The transient tire is part of the model for two reasons. A real tire builds its force over about one relaxation length d of rolling, while the force of Section 4 appears instantly. And the slip indices of Section 3.5 divide by the speed, so the belt could not be brought to rest; the transient tire removes that division. This section first gives the Maxwell model of A. De Felice [1] and then adds the damping of the carcass, which the model needs at low speed.

6.2 Maxwell model

Two viscoelastic analogues can describe the tire [1]. In the Kelvin–Voigt model a spring and a damper act in parallel, $F = Ku + c\dot{u}$. Under a constant sliding speed u grows without limit and so does the force, so the model has no steady state and cannot describe a rolling tire. In the Maxwell model they act in series, Figure 6.1, so they carry the same force and their displacements add,

$$F = Ku_k = c\,\dot{u}_c, \qquad u = u_k + u_c \qquad \Rightarrow \qquad \frac{c}{K}\,\dot{F} + F = c\,\dot{u} \tag{6.1}$$

Along x, u is the displacement of the rim relative to the road, so $\dot{u} = V_{sx}$, the slip velocity of Equation (3.5). The spring K is the carcass and u_k its deflection; the damper $c = C_s/|V_x|$ is the contact patch and u_c the distance it has slid. The point between them is the contact patch.

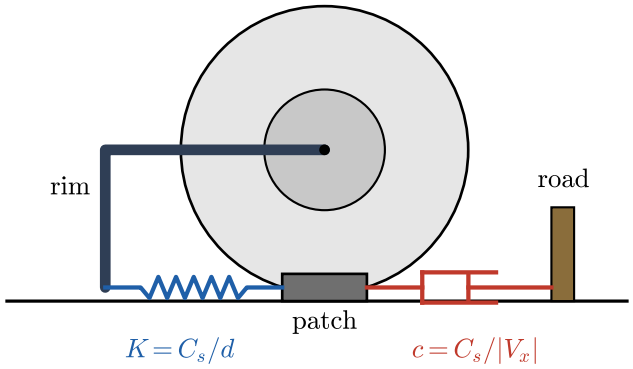


Figure 6.1. Maxwell model of the transient tire, side view along x; the element along y is the same. A rigid arm fixed to the rim, the carcass spring K, the contact patch, the contact damper c and the road.

Three steps turn Equation (6.1) into an equation in slips. First, the relaxation length is defined by $d = C_s/K$. Then $c/K = d/|V_x|$ and $c\,\dot{u} = C_s V_{sx}/|V_x|$.

$$\frac{d}{|V_x|}\,\dot{F} + F = C_s\,\frac{V_{sx}}{|V_x|} \tag{6.2}$$

Rolling forward, $V_{sx}/|V_x|$ is the practical slip s_x of Equation (3.6) and the right-hand side is $C_s s_x$, the form of A. De Felice [1]. Second, the force in the element is the spring force $F = Ku_k$. Divided by $C_s = Kd$ it becomes the carcass deflection divided by d, the *transient slip* $\tau_x = F/C_s = u_k/d$. It is written τ because it is neither the practical nor the theoretical slip; it is a deflection, not a ratio of velocities. Dividing by C_s,

$$\frac{d}{|V_x|}\,\dot{\tau}_x + \tau_x = \frac{V_{sx}}{|V_x|} \tag{6.3}$$

Third, multiplying by $|V_x|$ removes the division by the speed.

$$d\,\dot{\tau}_x + |V_x|\,\tau_x = V_{sx} \tag{6.4}$$

F acts along the sliding and the road pushes the tire the other way, so $F_x = -C_s\tau_x$. Along y the element is the same, with the same K and c, because the tire is isotropic. In vector form, with the characteristic for the size and Equation (4.2) for the direction [1],

$$d\,\dot{\boldsymbol{\tau}} + |V_x|\,\boldsymbol{\tau} = \mathbf{V}_s, \qquad \mathbf{F}_t = -\frac{\boldsymbol{\tau}}{\|\boldsymbol{\tau}\|}\,F_t(\|\boldsymbol{\tau}\|) \tag{6.5}$$

$\boldsymbol{\tau}$ is a state, zero at the start. The model holds for any sign of V_x and Ω, whether the wheel rolls forward or backward, is locked, or spins one way while moving the other. $\mathbf{V}_s$ is defined for every motion, and $|V_x|$ keeps the damper c positive; with the signed V_x a wheel moving backward would have $c < 0$ and $\boldsymbol{\tau}$ would grow without limit. The force always opposes the sliding. In steady state $\boldsymbol{\tau} = \mathbf{V}_s/|V_x|$, the practical slip $\mathbf{s}$ when rolling forward, which gives the force of Section 4. After a step in α the force builds up as $1 - e^{-\ell/d}$ with the distance ℓ rolled and reaches 63 % after one relaxation length, Figure 6.2, which takes 18 ms at 20 m/s.

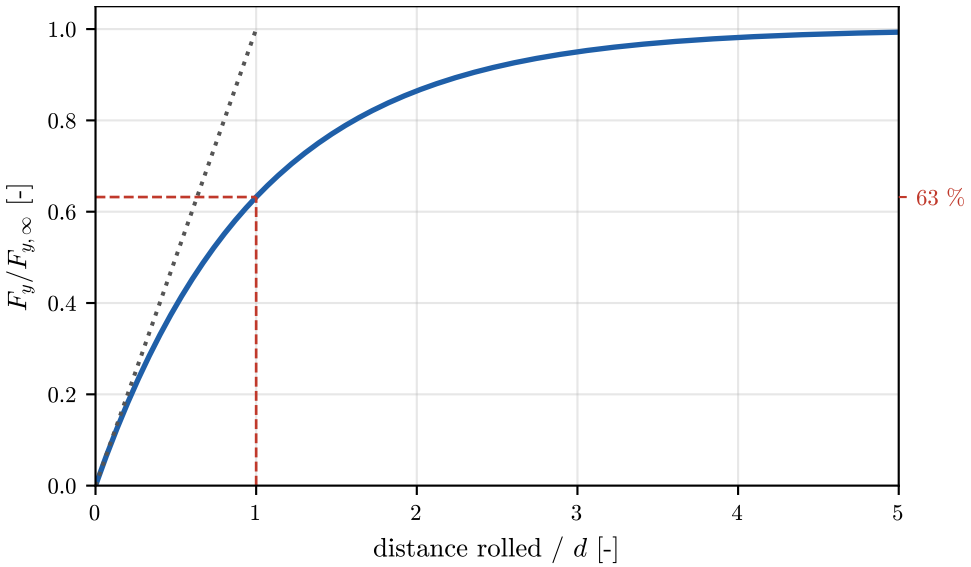


Figure 6.2. Build-up of the lateral force after a step in α, against the distance rolled divided by d. The force reaches 63 % of the steady value after one relaxation length.

6.3 Low-speed problem

As $V_x \to 0$, the damper c grows without limit and the patch cannot slide. Then $d\dot{\boldsymbol{\tau}} = \mathbf{V}_s$ and the tire is a pure spring, $\mathbf{F}_t = -K\mathbf{u}_k$. This is what lets the wheel stop and be held, but the spring has no damping. With the spin inertia J_w it forms a mode of natural frequency $\omega_n = \sqrt{KR_0h/J_w}$, about 19 Hz. A rotation of the rim deflects the carcass through R_0, Equation (3.5), and the force acts at the lever h. Its damping ratio is $|V_x|/(2d\,\omega_n)$, an estimate, which is 0.2 at 20 m/s, 0.01 at 1 m/s and zero at rest. A stopped wheel would oscillate on the tire indefinitely.

6.4 Carcass damping

A real carcass does not oscillate indefinitely, because its rubber dissipates energy; the Maxwell model has no element for this. A damper c_0 is therefore added in parallel with the spring, Figure 6.3. The carcass becomes a Kelvin–Voigt element in series with the damper of the contact patch. Along x both carry the same force and their displacements add.

$$F = Ku_k + c_0\,\dot{u}_k = c\,\dot{u}_c, \qquad u = u_k + u_c, \qquad \dot{u} = V_{sx} \tag{6.6}$$

The same three steps as in Section 6.2 apply. The patch slides at $\dot{u}_c = \dot{u} - \dot{u}_k$, so the carcass force equals $c(\dot{u} - \dot{u}_k)$.

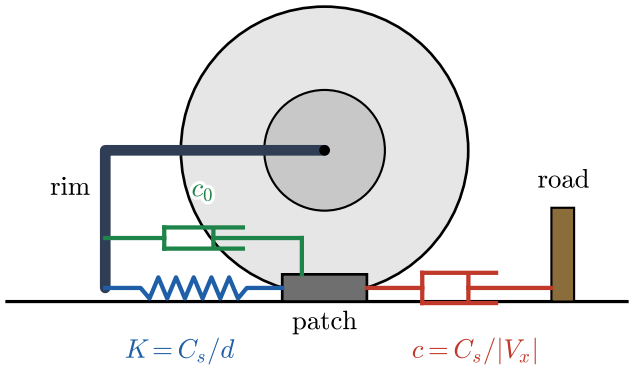


Figure 6.3. Transient tire with carcass damping, the model of Figure 6.1 with the damper c_0 in parallel with the carcass spring.

$$K u_k + c_0\,\dot{u}_k = c\,(\dot{u} - \dot{u}_k) \qquad \Rightarrow \qquad (c + c_0)\,\dot{u}_k + K u_k = c\,\dot{u} \tag{6.7}$$

Dividing by $c = C_s/|V_x|$ and using $K = C_s/d$, so that $c_0/c = c_0|V_x|/C_s$ and $K/c = |V_x|/d$,

$$\Big(1 + \frac{c_0|V_x|}{C_s}\Big)\dot{u}_k + \frac{|V_x|}{d}\,u_k = V_{sx} \tag{6.8}$$

Writing $u_k = d\,\tau_x$ as before gives

$$d\Big(1 + \frac{c_0|V_x|}{C_s}\Big)\dot{\tau}_x + |V_x|\,\tau_x = V_{sx} \tag{6.9}$$

In Section 6.2 the force was the spring force, $F = C_s\tau_x$. Now the carcass force also contains the damper, $F = K u_k + c_0\dot{u}_k = C_s\tau_x + c_0 d\,\dot{\tau}_x$. Divided by C_s it is the slip passed to the characteristic,

$$\tau_x^* = \frac{F}{C_s} = \tau_x + \frac{c_0 d}{C_s}\,\dot{\tau}_x, \qquad F_x = -C_s\tau_x^* \tag{6.10}$$

With $c_0 = 0$, $\tau_x^* = \tau_x$ and the equations reduce to those of Section 6.2. Along y the element is the same. In vector form, with the characteristic and the direction rule of Section 4,

$$d\Big(1 + \frac{c_0|V_x|}{C_s}\Big)\dot{\boldsymbol{\tau}} + |V_x|\,\boldsymbol{\tau} = \mathbf{V}_s, \qquad \boldsymbol{\tau}^* = \boldsymbol{\tau} + \frac{c_0 d}{C_s}\,\dot{\boldsymbol{\tau}}, \qquad \mathbf{F}_t = -\frac{\boldsymbol{\tau}^*}{\|\boldsymbol{\tau}^*\|}\,F_t(\|\boldsymbol{\tau}^*\|) \tag{6.11}$$

$\dot{\boldsymbol{\tau}}$ follows from the first equation, so there is no new state and no algebraic loop. c_0 is constant, so nothing in the model depends on a threshold speed. Three properties follow.

- In steady state $\dot{\boldsymbol{\tau}} = 0$, so $\boldsymbol{\tau}^* = \boldsymbol{\tau} = \mathbf{s}$, which gives the force of Section 4 unchanged by c_0 at any speed.
- In a transient the carcass deflects more slowly; the relaxation length becomes $d_{eff} = d\,(1 + c_0|V_x|/C_s)$.
- At rest $d\dot{\boldsymbol{\tau}} = \mathbf{V}_s$ and $\boldsymbol{\tau}^* = \boldsymbol{\tau} + (c_0/C_s)\mathbf{V}_s$, a spring and a damper in parallel. The 19 Hz mode then has the damping ratio $c_0\sqrt{R_0 h}/(2\sqrt{K J_w})$, an estimate.

6.5 Parameters

The relaxation length is the lateral value of the tire file [3], evaluated at the current load like the other tire parameters, A3,

$$d = p_{Ty1} \sin\Big(2 \arctan \frac{F_z}{p_{Ty2} F_{z0}}\Big) R_e \, \lambda_{Fz0} \tag{6.12}$$

with $p_{Ty1} = 2.144$, $p_{Ty2} = 1.983$ and $\lambda_{Fz0} = 0.81$, the scaling factor LFZO of the file, which PAC2002 applies here as a factor and again inside F_{z0}. At the reference load $d = 0.370$ m and $K = C_s/d = 143$ kN/m. The carcass damping $c_0 = 233$ N s/m is a design choice that gives the 19 Hz mode a damping ratio of about 0.10 at rest; there is no damping value for this tire.

The effective relaxation length grows with speed; d_{eff} is 2 % above d at 5 m/s, 9 % at 20 m/s and 26 % at 60 m/s. The value of the file belongs to a model without carcass damping, so it is a reference rather than the truth. Measured relaxation lengths are reported to grow with speed and load; whether the growth given by c_0 is realistic is a hypothesis, to be checked against a primary source and measured by S10 (limitation L10). One relaxation length is used in both directions, while the longitudinal value of the file is 0.54 m (limitation L11).

6.6 Growth of the transient slip in sliding

At $\delta = 90°$, $V_x = 0$, so Equation (6.11) only integrates $\mathbf{V}_s$. The force saturates correctly at $\mu_1 F_z$, but τ grows without limit, to $\tau_y = -54.1$ after 1 s in S8, a carcass deflection with no physical meaning. As $\|\boldsymbol{\tau}\|$ grows, the force along x per unit τ_x falls, so the carcass becomes an ever softer spring and the spin of a wheel sliding sideways with no torque dies out slowly, in 2.48 s, verified by S8. With any brake torque, or with δ steered to 90° gradually, the wheel stops within a fraction of a second. A limit on $\|\boldsymbol{\tau}\|$ would shorten the spin-down but change the force at large slip, so none is applied (limitation L14).

7 Numerical solution

7.1 State equations

The states are $\mathbf{q} = (\Omega, \tau_x, \tau_y)$, the inputs δ, T_D, T_B and the test conditions V and P, with $F_z = P + m_w g$ and the tire parameters at this load. At each time step the derivatives are evaluated in the order of Figure 7.1.

1. the wheel velocity V_x, V_y, Equation (3.1), and the slip velocity $\mathbf{V}_s$, Equation (3.5);
2. the derivative $\dot{\boldsymbol{\tau}}$, Equation (6.11);
3. the tire force $\mathbf{F}_t$ from $\boldsymbol{\tau}^*$, Equation (6.11) with Equation (4.5); the moments M_y, Equation (4.9), and M_z, Equation (4.11);
4. the spin derivative $\dot{\Omega}$ with the friction switch, Equations (5.7) and (5.9);
5. the hub actions and the belt forces, Equations (5.4) and (5.5);
6. the outputs for the display, α, R, $\mathbf{s}$ and $\boldsymbol{\sigma}$, Section 3.

There is no algebraic loop, because the forces depend only on the states, the inputs and the parameters.

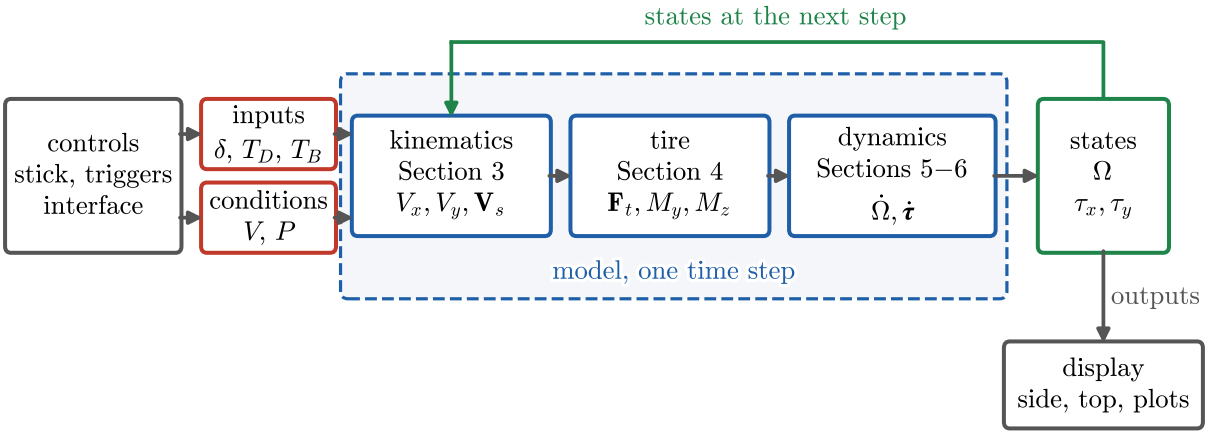


Figure 7.1. Data flow of one time step. The controls give the inputs and the interface the test conditions V and P; kinematics, tire and dynamics give the derivatives; the integrator gives the states of the next step; the display reads states and outputs.

7.2 Integrator and time step

The states are integrated with the classical fourth-order Runge–Kutta method at a fixed time step of 1 ms. The 19 Hz spin–tire mode of Section 6.3 is resolved easily at this step. The friction torque of Section 5.4 sets no limit, because it is constant while the wheel rolls. The fastest decay left is that of the transient slip, with the time constant $d_{eff}/|V_x|$, about 7 ms at 70 m/s at the reference load, an estimate.

The friction switch is evaluated once per step, from the state at its start. If $\Omega \neq 0$, $\nu = \text{sign}(\Omega)$ in all four stages of the step. If $\Omega = 0$, Equation (5.9) decides between a held wheel, with $\dot{\Omega} = 0$ in all stages, and a wheel that breaks free, with $\nu = \text{sign}(T_h)$. The derivatives are then smooth within the step, as the Runge–Kutta method requires. If Ω ends the step with the sign opposite to ν, the spin has passed through zero during the step. Ω is then set to zero only if the friction torque can hold the wheel there, that is if Equation (5.9) gives a held wheel at the end of the step; otherwise the spin keeps its value and the wheel turns on, as when it is reversed by the tire with no brake. A held wheel stays at exactly $\Omega = 0$, because every stage gives $\dot{\Omega} = 0$. Locking and release are detected with a delay of at most one step (limitation L7). The time step is confirmed by scenario S21; the integration stays stable up to 8 ms, Section 8.3.

7.3 Controls and reset

The inputs δ, T_D and T_B come from a game controller, the keyboard or the window, in one of two modes. In drive mode they follow the controls and return to zero when released, as in a car; the steer angle is limited to $\pm 20°$, a design choice. With the keyboard the arrows build the inputs up gradually, at a rate that grows with the time they are held, so the input grows with the square of that time: held from rest, a steer arrow reaches full lock in 0.5 s and the throttle or brake arrow T_{max} in 0.75 s. Released, the steer angle returns from full lock to zero in 0.4 s and the torque in 0.3 s. Drive mode is meant for a game controller, so the window recommends one when drive mode is chosen without it. In test mode, where the window opens, the inputs keep their value when released, so that steady conditions can be observed at any steer angle. The test conditions V and P are typed in the window; a new value changes only the test condition, Section 2.3.

Both torques are limited to $T_{max} = 1.1\, T_{lock}$, computed at the current load. The limit must lock and spin the wheel, with a margin small enough that the controls resolve the torque near T_{lock}. A reset returns the rig to free rolling at 10 m/s with $\delta = 0$ and no torque.

The window shows the rig in three dimensions and in side and top views with the vectors of Figures 2.1 and 2.2, the operating point on the characteristics of Section 4, the transient slip of Figure 6.3 and the free-body diagram of Figure 5.1. It only reads the outputs of Section 7.1 and computes no physics.

8 Verification plan

8.1 Reference values

Table 8.1 gives the values used by the acceptance criteria at the reference load; at other loads they follow from the same expressions with the tire parameters at that load. They are computed with rolling resistance neglected, an error of about 1.4 % on the torques, $f_0 F_z h / T_{lock}$. The locking torque is Equation (5.10).

Quantity	Expression	Value
locking torque	$T_{lock} \approx \mu_0 F_z h$	0.997 kN m
torque limit	$T_{max} = 1.1\, T_{lock}$	1.10 kN m
release of a locked wheel	$F_t(s{=}1)\, h = 0.996\, F_z h$	0.898 kN m
recovery from wheel spin	$\mu_1 F_z h = 0.942\, F_z h$	0.850 kN m
rolling drag in free rolling	$f F_z$	41.0 N
inertia force per belt acceleration	$J_w / (R_0 h)$	9.65 N per m/s^2
effective relaxation length at 20 m/s	$d\,(1 + c_0 \lvert V_x \rvert / C_s)$	0.402 m

Table 8.1. Reference values at the reference load, $F_z = 2.70$ kN.

8.2 Scenarios

Each scenario starts from free rolling at $V_0 = 20$ m/s unless stated otherwise. Each entry gives the inputs, then the acceptance criterion. The criteria compare with the equations or the reference values of Table 8.1; where a criterion gives no tolerance, the test states its tolerance as a design choice. S2, S6, S7, S10, S11, S14 and S15 run with M_y switched off, so that their criteria hold without the rolling drag; S19 and S20 state it themselves.

S1 Free rolling with $\delta = 0$ and no torque. Passes if $\Omega = V / R_0$ and $\mathbf{F}_t = 0$ without rolling resistance, and $F_x = -f F_z \approx -41$ N with it.

S2 Pure slip with $\delta \neq 0$ and no torque. Passes if $\Omega = \Omega_{0\alpha}$, $F_x \approx 0$, F_y lies on the characteristic Equation (4.5) with $s = \lvert \tan \alpha \rvert$ and the cornering drag is $F_{\parallel} = -F_y \sin \alpha$.

S3 Braking with a constant $T_B < T_{lock}$. Passes if the wheel reaches a steady point with $F_x = -(T_B + f F_z h)/h$ and $0 < s_x < s_p$, the slip at the peak.

S4 Locking with $T_B > T_{lock}$. Passes if Ω reaches zero and stays exactly there, Section 5.4, and $\mathbf{F}_t = -F_t(s)\, \mathbf{V}/V$ with $s = 1/\lvert \cos \alpha \rvert$, that is $0.996\, F_z$ at $\alpha = 0$, tending to $\mu_1 F_z$ as $\alpha \to 90°$.

S5 Driving with a constant $T_D < T_{lock}$. Passes if the wheel reaches a steady point with $F_x = (T_D - f F_z h)/h$ and $s_x < 0$.

S6 Wheel spin with $T_D > T_{lock}$. Passes if Ω grows without limit, since there is no engine model, and F_x falls from the peak toward the sliding force $\mu_1 F_z$.

S7 Combined slip, S3 or S5 with $\delta \neq 0$. Passes if (F_x, F_y) follows Equation (4.2) with Equation (4.5) for that α and never leaves the circle $\mu_0 F_z$.

S8 Sideways with $\delta = 90°$ and no torque. Passes if $V_x = 0$, $\Omega \to 0$ and $\mathbf{F}_t = -\mu_1 F_z\, \mathbf{V}/V$; the growth of τ is recorded to decide on its limit, Section 6.6.

S9 Reversed with $\delta = 180°$, then with T_D. Passes if $\Omega = -V/R_0$ without torque, and if with T_D the spin changes sign and $\sigma_x < -1$, as in Figure 4.5.

S10 Relaxation after a step in δ. Passes if τ_y reaches 63 % of its steady value after rolling d_{eff}, 0.402 m at 20 m/s. F_y then reaches about 66 %, because $\boldsymbol{\tau}^*$ adds the damper term, an estimate in the linear range.

S11 Stop with V ramped to 0, first with no torque, then with $T_B = T_{max}$. Passes if without torque the wheel comes to rest on the tire spring and the 19 Hz oscillation dies out with a damping ratio of about 0.10, and if with the brake the wheel locks, stays at $\Omega = 0$ and keeps the tire force it had when the belt stopped.

S12 Sweep with a slow ramp of δ. Passes if $F_y(\alpha)$ follows Equation (4.5) at the reference load and $M_z(\alpha)$ follows Equation (4.11) with the trail of Equation (4.12).

S13 Drive against brake with $T_D = T_B \leq T_{max}$. Passes with the result of S1, since the torques cancel while the wheel rolls, Equation (5.7).

S14 Lock and release, with T_B ramped slowly from 0 to T_{max} and back, then the same with T_D. Passes if the wheel locks above T_{lock} and rolls again only below 0.898 kN m, and spins above T_{lock} and recovers within 2 % above $\mu_1 F_z h = 0.850$ kN m, a design choice.

S15 Belt ramp with $\delta = 0$, no torque and V from 20 to 30 m/s in 1 s. Passes if during the ramp the tire spins the wheel up with $F_x = -J_w \dot{V}/(R_0 h) = -96.5$ N, within 1 %, reached after the relaxation lag.

S16 Start and standstill, with δ ramped at $V = 0$ and then V ramped from 0 to 20 m/s. Passes if the forces stay finite with no division by zero, α, $\mathbf{s}$ and $\boldsymbol{\sigma}$ are reported as undefined at $V = 0$, steering at rest gives no force, L12, and the run ends as S1.

S17 Through 180°, with δ swept through 180° at 60°/s and constant V. Passes if only δ wraps while Ω, $\boldsymbol{\tau}$, forces and moments stay continuous.

S18 Load cell, in four runs, combined braking at 5°, locking at 40°, driving at 160° and a belt ramp from 20 to 5 m/s. Passes if Equation (5.4) holds to rounding error and $F_\parallel^2 + F_\perp^2 = F_x^2 + F_y^2$.

S19 Falling branch, with M_y switched off, a constant T_B of 0.99 and 1.01 T_{lock}, and a start on the falling branch. Passes if the wheel settles below s_p at $0.99\,T_{lock}$, locks at $1.01\,T_{lock}$ and, started on the falling branch, leaves it, Section 5.5. Rolling resistance is switched off because it shifts the threshold by about 1.4 %, more than the margin of the test.

S20 No rolling resistance, S1 and S3 with M_y switched off. Passes if $F_x = 0$ and $\Omega = V/R_0$ in S1, and $F_x = -T_B/h$ in S3.

S21 Time step and load, S3, S4, S10 and S11 at 1, 0.5 and 0.25 ms, each at $F_z = 0.5$, 1.0 and $1.5F_{z0}$. Passes if steady values agree within 0.1 % and transients converge as the step halves; the largest stable time step is recorded.

S22 Power balance, in the four runs of S18. Passes if the power of motor and belt drive, $T_D\Omega - F_\parallel V$, equals the power of the friction torque, the rate of change of the kinetic energy $J_w\Omega\dot{\Omega}$ and the power taken by the tire, $-\mathbf{F}_t \cdot \mathbf{V}_s + F_x\Omega(h - R_0)$, to rounding error. The tire power is not split into carcass energy and dissipation, since with a nonlinear characteristic the split is not unique.

8.3 Results

Every scenario is implemented as a test in `tests/test_scenarios.py`, the tire values of Section 4 in `tests/test_tyre.py` and the window in `tests/test_interface.py`; all 61 tests pass. Table 8.2 compares measured and expected values for the scenarios with a quantitative result, printed by `tools/verification_values.py`. With `tools/time_step_check.py` the final values at 1 ms lie within 10^{-5} of those at 0.25 ms, and the integration stays stable up to 8 ms. One step costs about 30 µs, so the rig runs about 30 times faster than real time.

Scenario	Quantity	Expected	Measured
S1	rolling drag F_x	-41.0 N	-41.0 N
S4	locked force F_x/F_z	-0.996	-0.996
S4	time to lock at T_{max}	–	340 ms
S8	transient slip τ_y after 1 s	-54	-54.1
S10	distance to 63 % of τ_y	0.402 m	0.402 m
S10	F_y at that distance	0.662	0.662
S11	damping ratio at rest	0.0991	0.0991
S11	frequency at rest	19.3 Hz	19.3 Hz
S14	brake torque at locking	above 997 N m	1080 N m
S14	brake torque at release	below 898 N m	898 N m
S14	drive torque at spin recovery	850 to 867 N m	860 N m
S15	F_x during the belt ramp	-96.5 N	-97.3 N

Table 8.2. Verification results at the reference load.

In S14 the wheel locks well above T_{lock} because the brake torque is ramped and the slip grows slowly past the peak; the criterion is only that it cannot lock below T_{lock}. In S15 the force is 0.8 % above the estimate, which neglects the change of the slip with the belt speed.

9 Limitations and future work

9.1 Limitations

The assumptions A1 to A8 of Section 2.5 define the validity domain. Within it, the model has the following limitations.

L1 The vehicle loop is absent, so the tire force never changes the speed, §2.6.
L2 Longitudinal stiffness, peak and slip at the peak equal the lateral ones, §4.2.
L3 The rise of rolling resistance above the critical speed is absent, §4.6.
L4 The combined M_z ignores the longitudinal slip and the moment of F_x, §4.7.
L5 M_z for $|\alpha| > 90°$ lies outside the fitted range of the tire file, §4.7.
L6 Steering inertia and gyroscopic moment are neglected, §5.2.
L7 Locking and release are detected with a delay of at most one time step, §7.2.
L8 The falling branch of F_x cannot be measured under torque input, §5.5.
L9 Dive and squat are absent on the rig; they belong to the simulator, §5.5.
L10 The growth of the relaxation length with speed is not validated, §6.5.
L11 One relaxation length is used in both directions, §6.5.
L12 Steering a wheel at rest gives no force, as turn slip is not modeled, §8.2.
L13 The radii are fixed at the reference load, up to 3.5 % error on h in the load range, §5.1.
L14 A wheel sliding sideways with no torque stops spinning only after 2.5 s, §6.6.

9.2 Future work

The model leaves these effects out on purpose, and none of them is needed to implement the rig. They are described below in the order in which they are expected to be needed.

The first upgrades come with the simulator itself. There the chassis closes the vehicle loop, L1, and the wheel carrier rolls, pitches and steers, so the steering inertia and the gyroscopic moment, L6, and the dive and squat of the body, L9, enter the model. A powertrain, ABS and traction control follow. They rely on the brake holding a locked wheel, which the friction switch does

exactly. An optimiser that uses gradients would need a smooth friction law instead, since the switch makes the torque jump when the wheel locks or breaks free.

The tire law is then made more general. An anisotropic tire, with its own longitudinal stiffness, peak and slip at the peak, removes L2 and allows the longitudinal relaxation length of the tire file, L11. The combined-slip law of H. B. Pacejka [3] then replaces the friction circle and brings the full combined aligning moment, L4. In the vehicle, a spin with the pedals released shows whether the slow spin-down of L14 is visible; if it is, a limit on the transient slip is added. Camber with the overturning moment, A2 and A5, radii that follow the load and vertical dynamics, A3 and A4, and turn slip for steering at rest, L12, extend the validity domain. Temperature, pressure and wear, A8, come last.

Some values rest on a quoted source or a design choice and are checked before they are trusted. The coefficient K_f is checked against J. Y. Wong [4]; the carcass damping c_0 and the growth of d_{eff} with speed, L10, are compared with published measurements; the aligning moment beyond 90°, L5, is compared with a tire model fitted in that range. On the rig itself, an imposed spin would allow the falling branch of the longitudinal curve to be measured, L8.

9.3 Evidence gaps

The model is implemented and passes the scenarios of Section 8, Section 8.3. The scenarios check the model against its own equations; no value has yet been compared with a measured tire. The value of K_f is quoted from J. Y. Wong [4] and not yet checked against the book. The aligning moment beyond 90°, the value of c_0 and the growth of d_{eff} are hypotheses or design choices. The tests run on Linux, the interface tests off-screen; they have not yet run on Windows.

References

[1] A. De Felice, *Meccanica della ruota con pneumatico*, lecture notes, Università degli Studi di Modena e Reggio Emilia.

[2] Project Chrono, https://projectchrono.org, data of the sedan vehicle, with the tire file `Sedan_Pac02Tire.tir`, tire `Sedan_Pac02Tire.json` and rim `Sedan_Wheel.json`.

[3] H. B. Pacejka, *Tyre and Vehicle Dynamics*, 3rd ed., Butterworth-Heinemann, 2012.

[4] J. Y. Wong, *Theory of Ground Vehicles*, 4th ed., Wiley, 2008.

[5] Project Chrono, API reference, class `chrono::vehicle::ChBrakeSimple`, https://api.projectchrono.org.